NEOPLASIA
www.neoplasia.com

Volume 16 Number 10 October 2014 pp. 771–788 771

Tissue-Infiltrating Neutrophils Constitute the Major *In Vivo* Source of Angiogenesis-Inducing MMP-9 in the Tumor Microenvironment[1,2]

Elena I. Deryugina, Ewa Zajac, Anna Juncker-Jensen, Tatyana A. Kupriyanova, Lisa Welter and James P. Quigley

Department of Cell and Molecular Biology, The Scripps Research Institute, La Jolla, CA, USA

Abstract

According to established notion, one of the major angiogenesis-inducing factors, pro-matrix metalloproteinase-9 (proMMP-9), is supplied to the tumor microenvironment by tumor-associated macrophages (TAMs). Accumulated evidence, however, indicates that tumor-associated neutrophils (TANs) are also critically important for proMMP-9 delivery, especially at early stages of tumor development. To clarify how much angiogenic proMMP-9 is actually contributed by TAMs and TANs, we quantitatively evaluated TAMs and TANs from different tumor types, including human xenografts and syngeneic murine tumors grown in wild-type and *Mmp9*-knockout mice. Whereas host MMP-9 competence was required for full angiogenic potential of both normal and tumor-associated leukocytes, direct comparisons of neutrophils *versus* macrophages and TANs *versus* TAMs demonstrated that macrophages and TAMs secrete 40- to 50-fold less proMMP-9 than the same numbers of neutrophils or TANs. Correspondingly, the levels of MMP-9–mediated *in vivo* angiogenesis induced by neutrophils and TANs substantially exceeded those induced by macrophages and TAMs. MMP-9–delivering TANs were also required for development of metastasis-supporting intratumoral vasculature, characterized by ≥ 11-μm size lumens and partial coverage with stabilizing pericytes. Importantly, MMP-9–producing TAMs exhibit M2-skewed phenotype but do not express tissue inhibitor of metalloproteinases-1 (TIMP-1), a novel characteristic allowing them to secrete TIMP-1–free, neutrophil-like MMP-9 zymogen unencumbered by its natural inhibitor. Together, our findings support the notion whereby TANs, capable of immediate release of their pre-stored cargo, are the major contributors of highly angiogenic MMP-9, whereas tumor-influxing precursors of macrophages require time to differentiate, polarize into M2-skewed TAMs, shut down their TIMP-1 expression, and only then, initiate relatively low-level production of TIMP-free MMP-9 zymogen.

Neoplasia (2014) 16, 771–788

Introduction

Neutrophils and macrophages represent leukocytes with diversified functions in immune surveillance and inflammatory responses in tissues [1,2]. These two types of infiltrating leukocytes have also been implicated in regulating tumor development and angiogenesis [3–5], although the role of tumor-associated macrophages (TAMs) has been in a favored focus of cancer research for many years [6–9], whereas the critical functions of tumor-associated neutrophils (TANs) have only recently become appreciated [10–15].

Cancer metastasis depends on the induction of an angiogenic vasculature that in addition to nutrient supply provides structural conduits for tumor cell dissemination [16–18]. It has been demonstrated that matrix metalloproteinase-9 (MMP-9) plays a critical role in tumor angiogenesis and metastasis by turning on the angiogenic switch in

Abbreviations: BM, bone marrow; BMD, bone marrow–derived; CM, conditioned medium; IL, interleukin; KO, knockout; M-CSF, macrophage colony-stimulating factor; MMP, matrix metalloproteinase; PB, peripheral blood; PBD, peripheral blood–derived; TAM, tumor-associated macrophage; TAN, tumor-associated neutrophil; TIMP, tissue inhibitor of metalloproteinases

Address all correspondence to: E. Deryugina, PhD and J. Quigley, PhD, Department of Cell and Molecular Biology, The Scripps Research Institute, 10550 North Torrey Pines Road, La Jolla, CA 92037, USA. E-mails: deryugin@scripps.edu, jquigley@scripps.edu

[1] This article refers to supplementary materials, which are designated by Tables W1 to W5 and are available online at www.neoplasia.com.

[2] This study was supported by grants from National Institutes of Health R01CA105412 and R01CA129484. The authors declare no competing financial interests.
Received 12 July 2014; Revised 20 August 2014; Accepted 20 August 2014

1476-5586/14
http://dx.doi.org/10.1016/j.neo.2014.08.013

avascular tumors [19] and mediating the development and maintenance of distinct neovascular networks sustaining tumor cell intravasation [20]. Angiogenesis-inducing MMP-9 is supplied to the tumor microenvironment as a zymogen, proMMP-9, mostly by bone marrow–derived (BMD) myeloid cells, including TAMs and TANs [21], but the regulation of MMP-9 angiogenic activity remains unresolved.

Although a link between tumor-infiltrating leukocytes and their supplied MMP-9 has been shown [22–27], it has never been determined how much of proMMP-9 is actually contributed by a specific inflammatory cell type to tumor angiogenesis as well as what is the status or form of the delivered MMP-9. Depending on a particular cancer model, the angiogenesis-inducing MMP-9 was attributed to different types of tumor-infiltrating leucocytes. Thus, mast cells were shown to contribute their MMP-9 in the skin carcinogenesis model [22]. Pharmacological depletion of macrophages has emphasized a critical importance of TAMs in tumor growth and angiogenesis, mainly through vascular endothelial growth factor–involving mechanisms [28–31]. Furthermore, in the mouse model of cervical cancer, TAMs were credited with the supplementation of angiogenesis-switching proMMP-9 [32]. Accumulated evidence from our laboratory and others further indicated that neutrophils can more effectively supply their proMMP-9, which is uniquely free of tissue inhibitor of metalloproteinases-1 (TIMP-1), to potently induce angiogenesis in normal and pathophysiological environments [33–38].

Most recently, we have provided evidence that human M2 macrophages produce angiogenic proMMP-9, whereas M1 macrophages secrete low or non-angiogenic proMMP-9 [39]. Moreover, the angiogenesis-inducing capacity of proMMP-9 produced by M2 macrophages has been linked to its neutrophil-like, TIMP-free status since expression of TIMP-1 is rapidly and specifically shut down during M2 polarization [39]. This unique form of proMMP-9 secreted by physiologically normal M2 macrophages raised a cancer-related question regarding whether TAMs also produce TIMP-free proMMP-9 to induce angiogenesis within primary tumors, a notion that was directly addressed in this study. In addition, we thought to clarify whether TANs or TAMs, or both, serve as a main contributor of the angiogenic proMMP-9 within the tumor microenvironment.

By using a panel of murine and human tumors developing in MMP-9–competent and MMP-9–knockout mice (*Mmp9*-KO), we conducted quantitative biochemical, kinetic, and functional comparisons of TANs and TAMs and their proMMP-9. We have demonstrated that similar to inflammatory neutrophils and TANs, the proMMP-9 secreted by M2-skewed TAMs is TIMP-free, conferring it with angiogenesis-inducing capacity. Furthermore, although intact TANs and TAMs were both capable of inducing angiogenesis, the angiogenic potential of TAMs was much lower than that of TANs, which correlated with low levels of proMMP-9 secreted by TAMs even over long-time periods *versus* copious amounts released by TANs immediately on demand. Therefore, our data, which do not dispute the important role of TAMs in tumor development, nevertheless indicate that TANs constitute the dominant cell source of highly angiogenic proMMP-9. Thus, neutrophil MMP-9 might serve as a therapeutic target in human cancers in which early or chronic neutrophil infiltration is associated with enhanced tumor angiogenesis and poor prognosis.

Materials and Methods

Cell Lines and Culture Conditions

High- and low-disseminating variants of human prostate carcinoma, PC-hi/diss and PC-lo/diss [40], were generated from the parental cell line, PC-3, purchased from American Type Culture Collection (Manassas, VA). Murine L929 fibrosarcoma, B16-F10 melanoma (B16), and Lewis lung carcinoma (LLC) were from ATCC. All tumor cell lines were routinely tested and confirmed to be negative for mycoplasma and bacterial contamination and were used within 6 months after thawing low-passage frozen stocks. Tumor cells were cultured in Dulbecco's modified Eagle's medium (DMEM), supplemented with 10% FBS and 10 μg/ml gentamicin (D10), and passaged at confluence by a brief exposure to trypsin/EDTA.

Isolation of Murine Neutrophils from Peripheral Blood and Bone Marrow

All animal work was conducted in accordance to the animal protocol approved by the Institutional Animal Care and Use Committee of The Scripps Research Institute (TSRI, La Jolla, CA). Wild-type (WT) C57BL/6 mice were purchased from TSRI breeding colony at the age of 2 to 3 months. The *Mmp9*-KO mice on C57BL/6 background were purchased from Jackson Laboratories (Bar Harbor, ME) and bred at TSRI.

Murine neutrophils were isolated either from peripheral blood (PB) or bone marrow (BM of WT or *Mmp9*-KO C57BL/6 mice). Briefly, cardiac blood was collected into heparin-containing tubes and fractionated on a discontinued 1.007/1.119 Histopaque gradient according to the manufacturer's instructions (Sigma, St. Louis, MO). Alternatively, PB neutrophils were isolated with EasySep Mouse Neutrophil Enrichment kit from STEMCELL Technologies (Vancouver, Canada) according to the manufacturer's instructions. BM, providing a rich source of neutrophils [41], was flushed from femurs and tibias with DMEM–5% FBS. Single-cell suspension was generated by gentle pipetting and washed with Dulbecco's PBS. Then, neutrophils were purified by immunomagnetic isolation using biotinylated Ly6G mAb 1A8 (Biolegend, San Diego, CA) and streptavidin-conjugated magnetic beads (Miltenyi Biotec, San Diego, CA).

Isolated neutrophils were analyzed for purity by HEMA kit (Fisher Scientific, Kalamazoo, MI) and/or immunofluorescent staining with Ly6G mAb 1A8 (Biolegend). Isolated neutrophils with high levels of purity were used immediately in the angiogenesis assays or for release of their granule contents.

Generation of Murine Macrophages and Their Polarization

To generate BMD macrophages, BM was flushed from the femurs and tibias of WT or *Mmp9*-KO C57BL/6 mice. To generate PB-derived (PBD) macrophages, monocytes were isolated from cardiac blood with EasySep Mouse Monocyte Enrichment kit from STEMCELL Technologies according to the manufacturer's instructions. Murine BM cells and PB monocytes were plated onto tissue culture plates or Petri dishes at ~ 1×10^6 cells per 1 ml of RPMI 1640 supplemented with 10% FBS, 50 nM β-mercaptoethanol, and 10% conditioned medium (CM) from L929 fibrosarcoma cells, a rich source of macrophage colony-stimulating factor (M-CSF) [42]. Culture medium was changed for a fresh one every 2 to 3 days to generate mature M0 macrophages. On day 7, M1 phenotype was induced by exchanging M-CSF–containing medium for a mixture of 100 ng/ml lipopolysaccharide and 20 ng/ml interferon γ; M2 polarization was induced by 20 ng/ml recombinant murine interleukin-4 (IL-4) (PeproTech, Rocky Hill, NJ).

In Vivo Angiogenesis Assay

To determine the angiogenic capacity of intact cells or their secretates, we used a collagen onplant angiogenesis assay as described [43]. Briefly, intact cells or soluble proteins coming from equivalent number of cells (3×10^4/onplant) were incorporated into 2.1 mg/ml

neutralized native type I collagen (BD Biosciences, Franklin Lakes, NJ) and 30-μl collagen droplets were polymerized over gridded meshes, generating three-dimensional rafts (onplants) that were grafted onto the chorioallantoic membrane of chick embryos (five to six onplants per embryo). Phosphate-buffered saline (PBS) or serum-free (SF) medium was used as a negative control. To inhibit the proteolytic activity of murine MMP-9, recombinant murine TIMP-1 was incorporated at 4 ng per onplant. After 72 hours, the growth of newly developed blood vessels was recorded using a stereoscope. The levels of angiogenesis were determined as angiogenic indices calculated for each onplant as the ratio of number of grids with newly formed blood vessels *versus* total number of scored grids. The data are presented as fold difference of angiogenesis levels induced over PBS/SF medium control. Fold difference data from independent experiments were pooled and presented as means ± SEM.

Orthotopic Prostate Cancer Human Xenografts and Murine Tumors

Nonobese Diabetic/Severe Combined Immunodeficiency (NOD/SCID) mice were purchased from TSRI breeding colony at the age of 3 to 4 months. The PC-3 prostate cancer orthotopic xenografts were generated in NOD/SCID mice as described [40]. PC-lo/diss and PC-hi/diss cells were trypsinized, washed in D10 and then in SF DMEM, and resuspended in SF DMEM at 1×10^8 cells per ml. Immunodeficient male mice were anesthetized and approximately 10 μl of cell suspension (1×10^6 cells) was implanted into the anterior lobe of surgically exposed prostate gland. Within 3 to 6 weeks, the tumor xenografts were excised and either frozen on dry ice in the optimal cutting temperature compound (Sakura Finetek USA, Inc., Torrance, CA) or fixed in Zn-formalin (Fisher, Kalamazoo, MI) for histologic examination and immunostaining. The lungs were harvested and the levels of spontaneous metastasis of human tumor cells were determined by quantitative polymerase chain reaction detecting human-specific *Alu* repeats (*Alu*-qPCR) [40].

Murine tumors were generated by subcutaneous implantation of 5×10^5 cells into the flank of anesthetized mice. L929 tumors were grown in immunodeficient *nu/nu* mice, whereas B16 and LLC cells were implanted into the syngeneic wild-type (WT) or *Mmp9*-KO C57BL/6 mice. After tumors reached approximately 1 to 1.5 cm in diameter, the mice were sacrificed. Tumors were excised and either fixed in Zn-formalin for histologic examination, frozen on dry ice in the optimal cutting temperature solution for immunohistochemical analyses, or enzymatically digested to provide the source of TAMs and TANs.

Isolation and Characterization of TAMs and TANs

TAMs and TANs were isolated from murine tumors by magnetic bead separation according to the manufacturer's instruction (Miltenyi Biotec). The excised tumors were cut into small pieces and subjected to a mixture of bacterial collagenases I and IV and dispase (each at 1.0 mg/ml) and 1 unit/ml of DNase I (all from Sigma) in SF DMEM. Approximately 5 ml of enzymatic mixture were used for each gram of solid tumor. Cell dissociation was achieved by incubation for 1 to 2 hrs at 37°C, with occasional gentle agitation of the tube and pipetting of the contents through a 5-ml serological pipette. Dissociated tumor cells were washed once with D10, passed through 70-μm nylon mesh strainer (BD Biosciences), and then washed twice with PBS, pH 7.2, supplemented with 1% BSA (PBS-BSA; passed through a 0.22-μm filter). When indicated, cell pellet was subjected to red blood cell lysis and then washed in PBS-BSA. For TAM and TAN isolations, single-cell suspensions at 4×10^7 cells per ml were incubated with 10 μg/ml biotin-conjugated F4/80-specific or Ly6G-specific mAbs, respectively (both mAbs from Biolegend). After 1-hour incubation on ice with occasional agitation, the cells were washed twice with PBS-BSA and incubated at 1×10^8 cells per ml with streptavidin-conjugated magnetic microbeads (Miltenyi Biotec) at 9:1 (vol/vol) ratio. Cells were washed once with ice-cold PBS-BSA, filtered through 40-μm nylon mesh strainer, and applied, under magnetic field, to pre-washed Miltenyi Macs separation LS columns at 5×10^7 to 10×10^7 cells per 0.5 ml per column. Columns were washed five times with 1 ml of PBS-BSA and flow-through fraction was collected for further analyses. To elute magnetically separated cells, the columns were removed from magnetic field and flushed with 6 ml of PBS-BSA. Eluted cells were washed and subjected to further analyses.

Details on TAM and TAN isolations and their characterization by flow cytometry are presented in the Supplementary Data file (see Appendix A). The isolated cells with high purity (90-95%) were used immediately in the *in vivo* angiogenesis assays and/or used for accumulation of their respective secretates.

Generation of Neutrophil Releasates and Macrophage CM

Isolated neutrophils and TANs were induced to release their proMMP-9 by incubation at 0.5×10^7 to 1.0×10^7 cells per ml PBS for 1 hour at 37°C. The releasates were cleared from the cell ghosts by centrifugation at 14,000 rpm for 10 minutes at 4°C and frozen in aliquots at − 80°C until use.

Isolated macrophages and TAMs were incubated in tissue culture plates at 1×10^6/ml, first in D10 to allow the cells to adhere to plastic, and then in SF DMEM to collect CM at 48 hours. Alternatively, TAMs were kept D10, and the cells were analyzed for lineage-specific markers by flow cytometry after 2- to 5-day incubation.

Statistical Analysis and Data Presentation

Statistical analyses were performed using Prism Software (GraphPad, San Diego, CA). In bar graphs, data are presented as means ± SEM from a representative experiment or several normalized experiments, in which fold changes were calculated from the pooled fold differences by taking ratios of numerical values for individual measurements in experimental groups over the mean of control group. The unpaired two-tailed Student's *t* test was used to determine significance ($P < .05$) in difference between data sets.

Supplementary Data

Supplementary Data file (see Appendix A) contains detailed information on well-established procedures employed in this study, including Western blot analysis, immunohistochemistry, cytologic and immunofluorescent analyses of isolated cells, flow cytometry analysis of TAMs for cell surface markers, gelatin zymography, and gene expression analysis by real-time quantitative reverse transcription–PCR analysis.

Results

MMP-9 Production by Murine Neutrophils and Macrophages

In preparation for an extensive *in vivo* analysis of MMP-9 production by TANs and TAMs, we initially investigated and quantified MMP-9 production by normal murine mature neutrophils *versus* macrophages. Double staining of non-fractionated PB indicated that Gr-1–positive neutrophils manifest high levels of MMP-9, whereas Gr-1–negative mononuclear cells appear MMP-9 negative (Figure 1*A*). Neutrophils were isolated from PB and their purity was validated by HEMA staining (Figure 1*B*, *left*) and Ly6G-specific immunofluorescent staining with

mAb 1A8 (Figure 1*C*, *left*). Alternatively, the neutrophils were isolated from BM, which provided a rich source of highly purified mature granulocytes (Figure 1*B*, *middle*). Since murine PB has low numbers of monocytes, BM was also used to generate murine macrophages. Adherent BM cells were cultured in the presence of murine M-CSF to induce macrophage differentiation and maturation, which was indicated by HEMA staining after 7- to 9-day incubation (Figure 1*B*, *right*). Immunofluorescent analysis validated that M-CSF–induced BM cells were represented by almost 100% of F4/80-positive macrophages (Figure 1*C*, *right*).

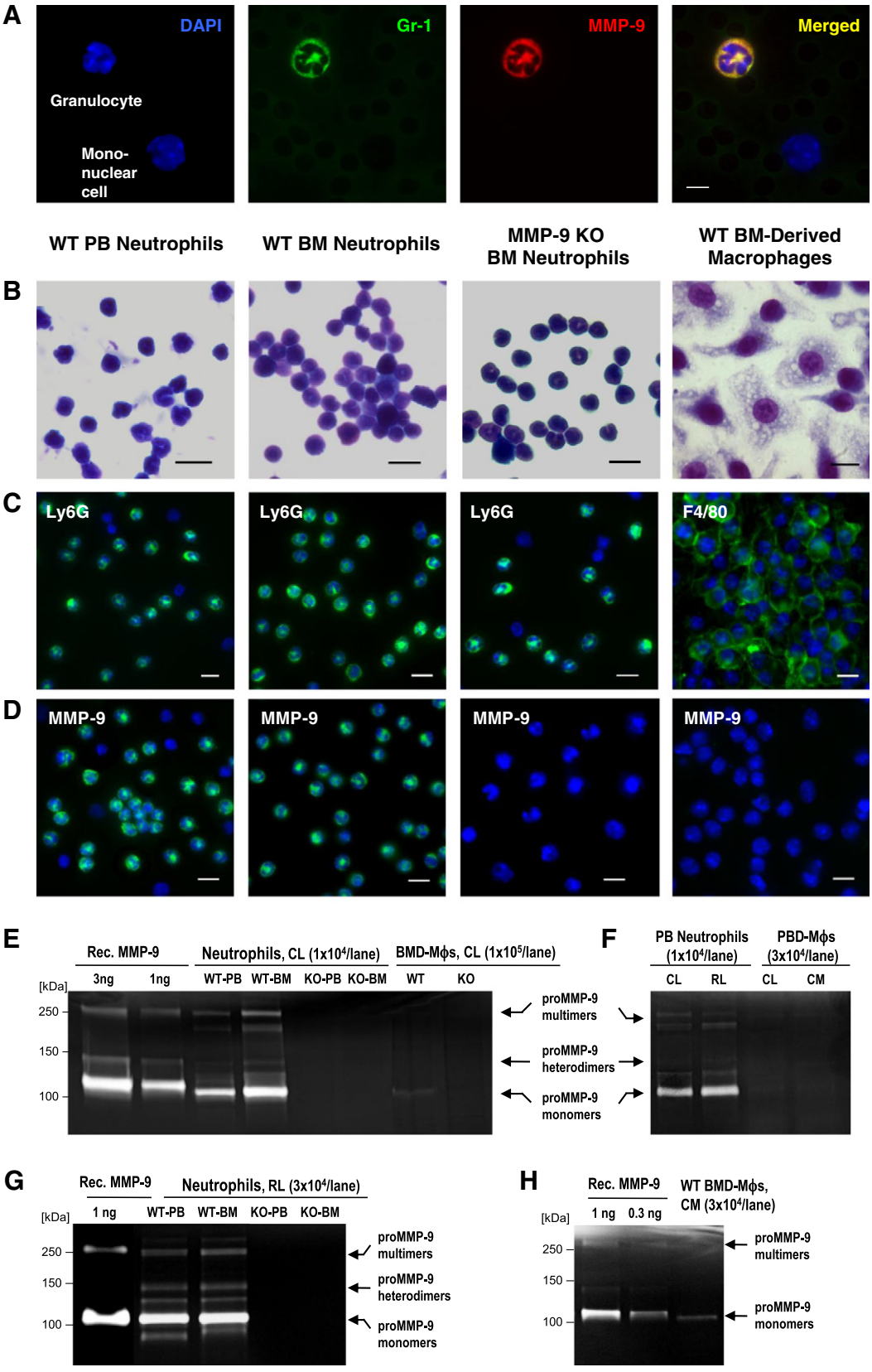

In agreement with the natural accumulation of MMP-9 in their secretory granules, the intact neutrophils, isolated from either PB or BM of WT mice, were brightly stained for murine MMP-9, whereas no positive immunofluorescence for MMP-9 was detected in Ly6G neutrophils isolated from the BM of *Mmp9*-KO mice (Figure 1*D*). In contrast to WT neutrophils, WT BMD macrophages did not generate any significant MMP-9 signal (Figure 1*D*, *right*).

Cell lysates from PB and BM neutrophils and BMD macrophages were subjected to gelatin zymography to compare their levels of *intracellular* MMP-9. Neutrophils contained MMP-9 in its zymogen form, proMMP-9, represented by ~105-kDa monomers, ~130-kDa heterodimers of proMMP-9 with NGAL, and higher molecular weight complexes of an apparent molecular weight of ~270 kDa (Figure 1*E*). Quantitative comparisons against known amounts of recombinant murine proMMP-9 demonstrated that 1×10^6 of PB and BM neutrophils accumulated up to 112.5 ± 17.7 ng ($n = 2$) and 88.9 ± 6.8 ng ($n = 3$) of proMMP-9, respectively. In contrast, lysed BMD macrophages produced very weak gelatinolytic bands (Figure 1*E*), corresponding to only 1.2 ± 0.5 ng ($n = 3$) of proMMP-9 per 1×10^6 cells, which represents less than 2% of MMP-9 stored in equivalent number of neutrophils. Confirming MMP-9 nature of the zymographic bands, neutrophils isolated from PB and BM of *Mmp9*-KO mice as well as macrophages derived from BM of *Mmp9*-KO mice did not show any gelatinolytic bands (Figure 1*E*).

We next examined whether PB monocytes would differentiate into macrophages capable of higher levels of MMP-9 than their BMD counterparts. Isolated PB mononuclear cells were incubated with M-CSF for 9 days to yield mature F4/80-positive macrophages. However, these PBD macrophages also induced extremely low MMP-9 gelatinolytic activity in comparison to PB neutrophils (Figure 1*F*).

The amounts of proMMP-9 *secreted* by macrophages were compared with those *released* by neutrophils. Quantitative zymographic analyses demonstrated that 1×10^6 neutrophils from PB and BM released, respectively, 61.1 ± 11.9 ng ($n = 9$) and 70.0 ± 13.7 ng ($n = 5$) of proMMP-9 within 1 hour, whereas the same number of BMD or PBD macrophages secreted only 4.4 ± 2.6 ng ($n = 4$) and 2.5 ± 0.4 ng ($n = 2$) of proMMP-9 during a 2-day-long incubation (Figure 1, *F–H*). Therefore, tissue-resident macrophages would require at least 30 days for producing the same amount of proMMP-9 releasable by neutrophils immediately on demand.

Together, these findings indicate that tissue-infiltrating neutrophils can rapidly provide a rich source of proMMP-9 required for inducing angiogenic responses *in vivo*. In contrast, tissue-resident macrophages might need prolonged time to synthesize and secrete their proMMP-9 to reach even threshold concentrations required for angiogenic stimulation.

MMP-9–Mediated Angiogenesis Induced In Vivo by Neutrophils and Macrophages

Angiogenic potential of murine neutrophils and macrophages and their proMMP-9 was analyzed in the well-established quantitative assay involving live chick embryos grafted with three-dimensional collagen onplants [43]. The angiogenic potential of mature BMD macrophages (M0 phenotype) was quantified in comparison with their M1- and M2-polarized counterparts. Whereas intact neutrophils induced high levels of angiogenesis at 4.6 ± 0.9 fold excess *versus* no cell control ($P < .0001$), fully differentiated M0 macrophages were only moderately angiogenic, demonstrating a 2.2 ± 0.3 fold excess over negative control ($P < .0001$; Figure 2*A*). Furthermore, angiogenesis-inducing capacity of intact neutrophils but not M0 macrophages almost entirely depended on their MMP-9 competence (Figure 2*A*).

Acquisition of M1 phenotype after interferon γ/lipopolysaccharide treatment did not change significantly the relatively low angiogenic capacity of M0 macrophages. Importantly, angiogenic potentials of M0 and M1 macrophages from *Mmp9*-KO mice were similar to those of their WT counterparts (Figure 2*A*), indicating that low angiogenesis-inducing capacity of these two macrophage phenotypes was independent of MMP-9 production. In contrast, induction of M2 phenotype resulted in a significant increase of the angiogenic capacity of the IL-4–treated M0 macrophages reflected in 3.1 ± 0.4 fold excess over no cell control ($P < .0001$). Furthermore, M2 macrophages from *Mmp9*-KO mice demonstrated a low angiogenic potential, comparable to that of MMP-9–deficient M0 and M1 macrophages (Figure 2*A*). These findings point out that the enhanced angiogenesis-inducting capacity of MMP-9–competent M2 macrophages was entirely dependent on their ability to produce MMP-9 and thus providing one of the molecular explanations for the known proangiogenic potential of M2-polarized macrophages.

Remarkably close patterns were observed between the angiogenesis levels induced by intact cells and their respective secretates (Figure 2, *A* and *B*). Thus, the levels of angiogenesis induced by neutrophil releasates were comparable to those induced by intact cells, including the dependence on MMP-9 since neutrophil releasates from Mmp9-KO mice induced angiogenesis at no-cell control levels (Figure 2*B*). Similar to the pattern observed with intact macrophages, the M0 and M1 secretates were only low to moderately angiogenic and independent of their genetic ability to generate proMMP-9 (Figure 2*B*). In contrast, the M2 macrophage secretate induced enhanced levels of angiogenesis, exceeding 3.6 ± 0.4 fold the negative control ($P < .0001$) and demonstrating entire dependence on MMP-9 genetic status (Figure 2*B*).

To correlate the levels of angiogenesis-inducing activity with the levels of produced MMP-9 protein, we quantified proMMP-9 content in BM neutrophil releasates and secretates of M0, M1, and M2 BMD macrophages by Western blot analysis. Within 2-hour induction, 1×10^6 of WT neutrophils released 164.1 ± 48.1 ng of proMMP-9 ($n = 7$), but surprisingly, the same number of M0, M1, and M2 macrophages during a 48-hour-long incubation produced only 4.8 ± 2.2 ($n = 4$), 11.5 ± 2.7 ($n = 8$), and 8.6 ± 2.1 ng ($n = 9$) of proMMP-9, respectively (Figure 2*C*, *top*), which represents only 3% to 7% of that released on demand by neutrophils.

Figure 1. Normal neutrophils are the major producer of MMP-9. (A) Unfractionated PB from WT mice was immunostained for Gr-1 (green) and MMP-9 (red). Cell nuclei were highlighted with 4',6-diamidino-2-phenylindole dihydrochloride (blue). Bar, 5 μm. (B–D) Neutrophils were isolated from PB or BM of WT or *Mmp9*-KO mice, whereas macrophages (Mφs) were generated from adherent BM mononuclear cells. Bars, 10 μm (B) HEMA staining. (C) Immunostaining (green) for Ly6G or F4/80. (D) Immunostaining *(green)* for MMP-9. (E–H) Zymographic analysis of MMP-9. Recombinant murine proMMP-9 (Rec. MMP-9) provided standards for quantification of MMP-9. Arrows point to the 105-kDa monomers, ~130-kDa heterodimers, and ~270-kDa multimers of proMMP-9. (E) Cell lysates (CL) of BMD-Mφs and neutrophils isolated from PB or BM of WT or *Mmp9*-KO mice. (F) CL and releasates (RL) from WT PB neutrophils and CL and CM from WT PBD-Mφs. (G) RL from PB and BM neutrophils isolated from WT and *Mmp9*-KO mice. (H) CM from WT BMD-Mφs.

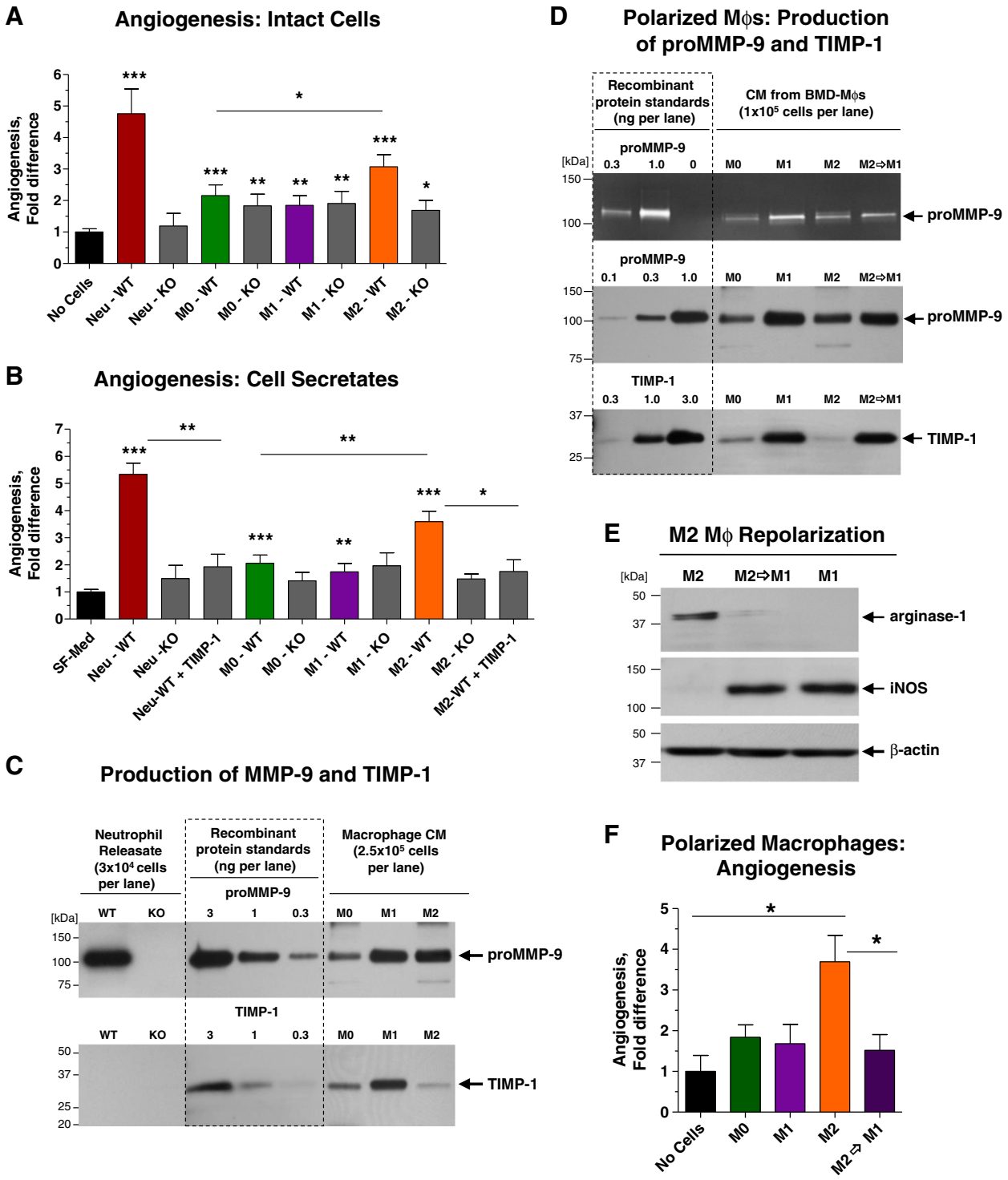

Figure 2. Angiogenic potential of neutrophils and M2 macrophages depends on production of proMMP-9. (A and B) Neutrophils and macrophages (Mφs), derived from WT and *Mmp9*-KO BM, were analyzed for their angiogenic potential *in vivo* as intact (3×10^4) cells (A) or their secretates (B). Mature BMD-Mφs (M0 phenotype) were polarized toward the M1 or M2 phenotype. In (B), recombinant TIMP-1 was added to WT neutrophil releasate and M2 Mφ CM. Pooled data from three (A) and seven (B) independent experiments, each employing from four to six embryos grafted with four to six onplants per variant, are presented. Data are means ± SEM. $^*P < .05$, $^{**}P < .005$, $^{***}P < .0001$. (C) Western blot analysis of MMP-9 (top) and TIMP-1 (bottom) produced by BM neutrophils and BMD-Mφs was performed in comparison with recombinant proMMP-9 (105 kDa) and TIMP-1 (28 kDa) standards. (D) Zymographic (top) and Western blot analyses of MMP-9 (middle) and TIMP-1 (bottom) secreted by Mφs were performed in comparison with recombinant proMMP-9 (105 kDa) and TIMP-1 (28 kDa) standards. Mature M0 Mφs were polarized toward the M1 or M2 phenotype. A portion of M2 Mφs was then reversed toward the M1 phenotype. (E) Analysis of arginase-1 and iNOS expression in M1, M2, and M2→M1 repolarized Mφs. (D) Angiogenic potential of mature, polarized, and repolarized Mφs was determined *in vivo* as described in A. One of two independent experiments employing from five to seven embryos, each grafted with four to six onplants per variant, is presented. Bars are means ± SEM. $^*P < .05$.

Angiogenic Capacity of Neutrophils and M2 Macrophages Depends on Their Production of TIMP-1–Free proMMP-9

Since both the activation of human proMMP-9 and the functional angiogenic activity of the resultant enzyme depend on the levels of TIMP-1 bound to the zymogen [34,36,38], we quantified how much TIMP-1 was produced by *murine* neutrophils and macrophages (Figure 2*C*, *bottom*). In agreement with the known lack of TIMP-1 expression in neutrophils [44], no TIMP-1 was detected in neutrophil releasate. In contrast, M0 and M1 macrophages produced TIMP-1 at levels exceeding the 1:1 stoichiometric MMP-9/TIMP-1 molar ratio, suggesting the production of proMMP-9 fully complexed with TIMP-1. However, polarization to M2 phenotype was accompanied by a remarkable reduction of TIMP-1, indicating that murine M2 macrophages secreted TIMP-deficient, angiogenic proMMP-9. Consistent with this notion, the addition of exogenous TIMP-1 to M2 secretate reduced its angiogenesis-inducing capacity down to the levels of the *Mmp9*-KO M2 cells. Similarly, the angiogenesis-inducing capacity of TIMP-free WT neutrophil releasate was also highly sensitive to TIMP-1 addition ($P < .005$; Figure 2*B*).

To confirm that production of TIMP-1 is detrimental for the ability of macrophages to induce angiogenesis, M0 macrophages were first polarized toward M1 or M2 phenotypes, and then the M2 macrophages were repolarized toward M1 phenotype or kept in M2 state (Figure 2*D*). Consistent with the reciprocal pattern of inducible nitric oxide synthase (iNOS) and arginase-1 expression in M1/M2 macrophages, M2→M1 repolarization resulted in the induction of iNOS and disappearance of arginase-1 (Figure 2*E*). M2→M1 repolarization was not accompanied by any significant changes in the production of proMMP-9 but resulted in a dramatic induction of TIMP-1 (Figure 2*D*), expressed at levels characteristic of M1 macrophages. Importantly, M2→M1 repolarized macrophages completely lost their enhanced angiogenic capacity and were angiogenic only at the low background levels exhibited by M1 macrophages (Figure 2*F*).

Together, these results demonstrate that both neutrophils and M2 macrophages uniquely produce TIMP-deficient proMMP-9, and therefore, these two types of leukocytes can provide the angiogenic MMP-9 to the sites of tissue inflammation, including sites of tumor development.

TANs and TAMs in Human Prostate Cancer Xenografts

Relative contribution of TANs and TAMs to tumor angiogenesis and metastasis was initially investigated in human prostate cancer xenografts grown in NOD/SCID mice. Human prostate cancer PC-3 variants, PC-hi/diss and PC-lo/diss, selected *in vivo* for high and low dissemination capacities [40], were implanted into anterior prostates. At 6 weeks, the mouse lungs were analyzed for levels of spontaneous metastasis, whereas primary tumors were processed for quantitative analyses of inflammatory leukocyte influxes as well as angiogenesis (Figure 3, *A* and *B*). Human-specific *Alu*-qPCR confirmed the significant differential between the levels of lung metastasis in PC-hi/diss *versus* PC-lo/diss variants (Figure 3*B*, *left*). Whereas similar densities of F4/80-positive TAMs were observed between PC-lo/diss and PC-hi/diss tumors, the density of Ly6G-positive TANs was approximately 2.5- to 3.0-fold higher within PC-hi/diss xenografts compared with PC-lo/diss counterparts (Figure 3, *A* and *B*, *middle*). This differential in the TAN density was concomitant with a three-fold differential in the density of lumen-containing angiogenic vessels in PC-lo/diss *versus* PC-hi/diss xenografts (Figure 3, *A* and *B*, *right*), thus linking the levels of inflammatory neutrophils with the levels of tumor angiogenesis.

A significant 5.5-fold differential in the density of TANs *versus* TAMs was also validated in PC-hi/diss tumors at 3 weeks (Figure 3*C*), consistent with the notion that neutrophil influx and delivery of highly angiogenic neutrophil MMP-9 at early times were associated with the induction of tumor angiogenesis and development of a metastasis-sustaining vasculature. Double staining of PC-hi/diss tumor sections for murine MMP-9 along with either neutrophil-specific Ly6G or macrophage-specific F4/80 indicated that leukocyte MMP-9 was associated almost exclusively with neutrophils and not with macrophages (Figure 3*D*). Thus, almost 100% of Ly6G-positive TANs manifested significant overlap of their cell-specific 1A8 signal with the MMP-9–specific signal (Figure 3*D*, *top*). Murine MMP-9 was also found associated with stromal fibrillar material localized between tumor cells and, almost invariably, in the areas of neutrophil congregation. In contrast, F4/80-positive TAMs demonstrated no direct overlap with MMP-9 even in the areas of MMP-9–positive matrix localization (Figure 3*D*, *bottom*). Quantitative analysis indicated that 96.6 ± 2.3% ($n = 3$) of all MMP-9–positive tumor-associated leukocytes were TANs, whereas almost 100% of TAMs were negative for MMP-9, supporting the notion that TANs are the main suppliers of angiogenesis-inducing MMP-9.

Biochemical and Functional Characterization of L929 TAMs and Their Secreted MMP-9

To further investigate whether TANs or TAMs supply the majority of angiogenesis-inducing proMMP-9 to the tumor microenvironment, we compared the angiogenic capabilities of TAMs and TANs isolated from a number of syngeneic mouse tumors. We initially generated L929 tumors because L929 fibrosarcoma cells produce large amounts of the monocyte/macrophage attractant, M-CSF [42]. L929 tumors developed a robust network of angiogenic vessels and capillaries and also recruited inflammatory cells that accumulated at the tumor border and in islands within tumor interior (Figure 4*A*). Immunofluorescent staining of L929 tumors for leukocyte-specific antigens illuminated large, island-like congregations of F4/80-positive macrophages but only few Ly6G-positive neutrophils (Figure 4*B*), and therefore L929 tumors were used to purify only TAMs.

L929 tumors yielded on average 29.0 ± 5.4 × 10^6 TAMs per 1 × 10^8 cells of initial cell suspension (Table W1), indicating an extremely high percentage of TAMs in this murine tumor type likely due to overexpression of M-CSF. Flow cytometry of freshly isolated and *in vitro* cultivated L929 TAMs confirmed their high purity by staining for myeloid cell and macrophage antigens, including CD11b, CD206/MMR, and F4/80 (Tables W1 and W2). L929 TAMs also expressed high levels of arginase-1 and were negative for iNOS (Figure 4*C*), a dual characteristic indicating an M2-skewed phenotype of isolated TAMs. M2-skewed phenotype of L929 TAMs was also corroborated by gene expression analysis, which showed that while L929 tumor cells were negative for *Arg1* and *Mrc1*, isolated L929 TAMs exhibited high expression levels of these two genes characteristic of M2 macrophages (Figure 5*A*). Relatively high levels of *Agr1* and *Mrc1* were also observed within dissociated tumors (Figure 5*A*), consistent with high TAM representation in the M-CSF–enriched L929 tumors.

Western blot analysis demonstrated that while original L929 tumor cells did not produce any detectable levels of proMMP-9 or TIMP-1,

the isolated L929 TAMs secreted proMMP-9 but no detectable TIMP-1 (Figure 5*B*). Densitometry analyses indicated that 1×10^6 L929 TAMs secreted 3.4 ± 1.3 ng of TIMP-free proMMP-9 within 48-hour incubation ($n = 6$).

Although intact L929 TAMs induced moderate levels of angiogenesis, their secreted products induced higher angiogenic levels (2.7 ± 0.5 fold, $P < .05$ *versus* 4.3 ± 0.7 fold increase, $P < .001$, respectively) (Figure 5*C*). This enhanced angiogenesis-inducing activity of CM was sensitive to exogenous TIMP-1 (Figure 5*C*), indicating that the accumulated TIMP-free proMMP-9 was responsible for the higher levels of angiogenesis induced by L929 TAM CM.

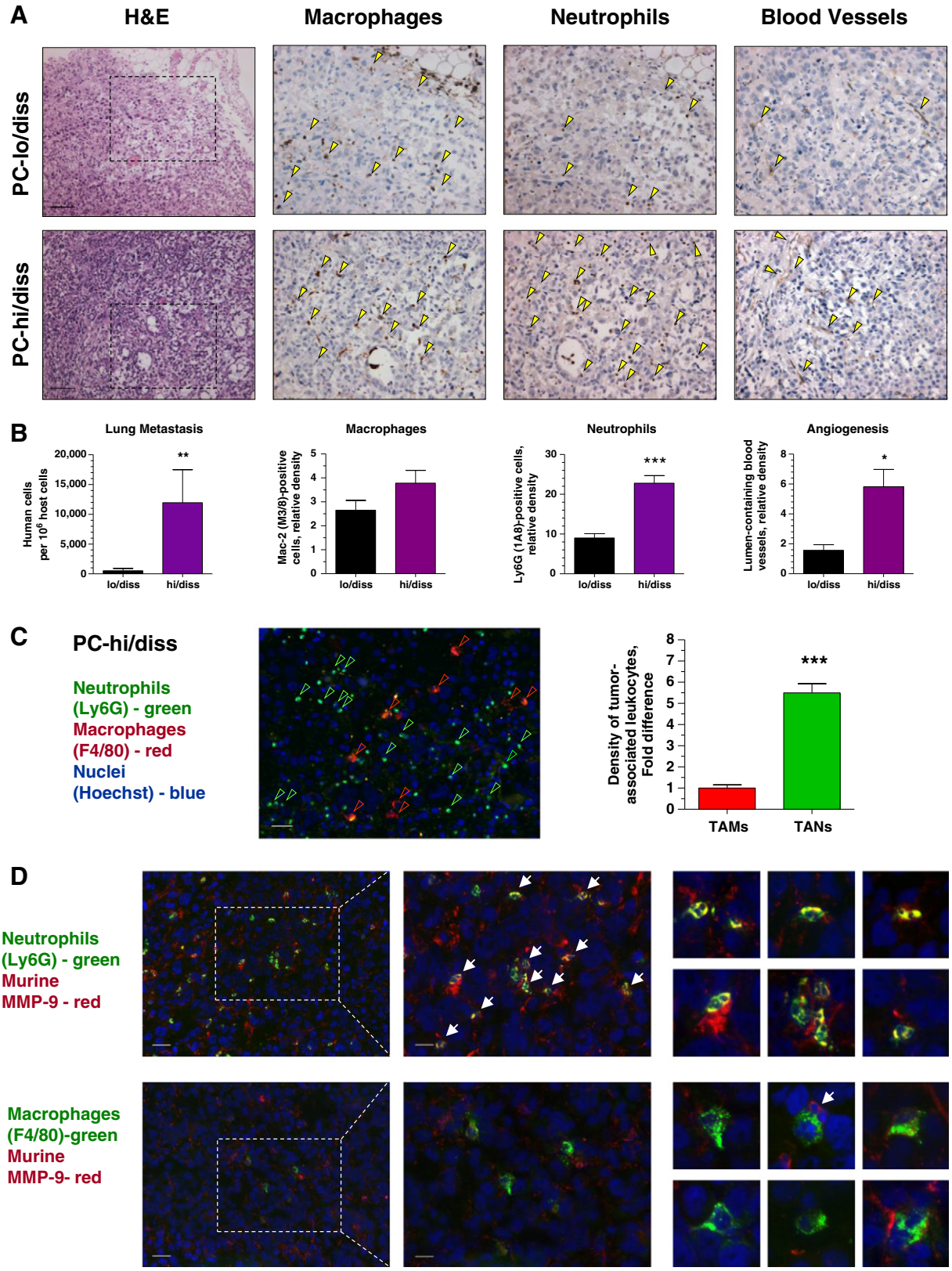

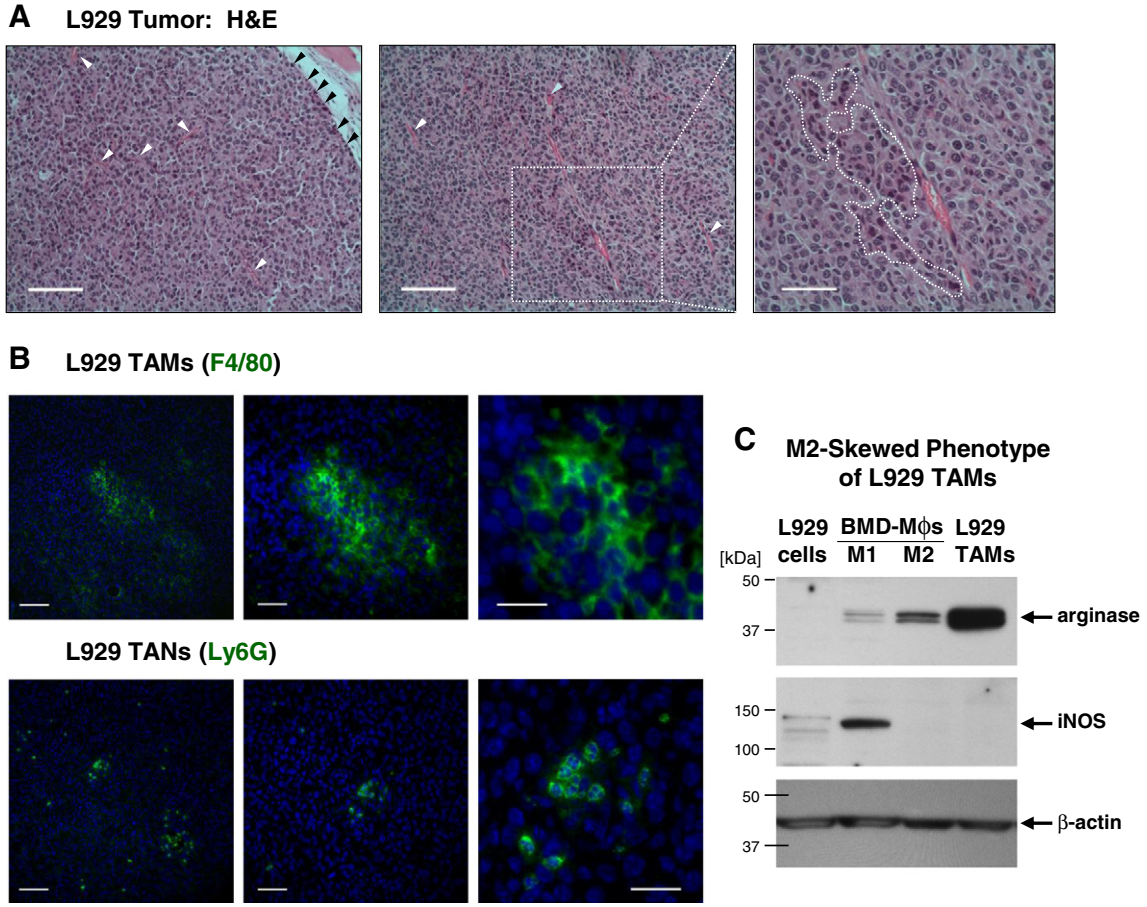

Figure 4. TAMs and TANs in murine L929 tumors. (A) Left: Outer portion of L929 tumor depicting tumor-stroma border infiltrated with leukocytes (black arrowheads). Several blood vessels are indicated by white arrowheads. Bar, 100 μm. Middle: Inner portion of the same L929 tumor depicting lumen-containing blood vessels, some with neutrophils (blue arrowhead). Bar, 100 μm. Right: An island of macrophage-like leukocytes characterized by dark blue–stained nuclei and highly eosinophilic cytoplasm is outlined. Bar, 50 μm. (B) L929 TAMs (top) and TANs (bottom) highlighted by immunofluorescent staining (green) for F4/80 and Ly6G, respectively. Images to the right depict areas examined at increasing magnifications. Bars, 100 μm, 50 μm, and 25 μm in left, middle, and right panels, respectively. (C) Western blot analysis of L929 TAMs for expression of arginase-1 and iNOS. Parental L929 tumor cells and L929 TAMs analyzed in comparison with the lysates of WT M1 or M2 polarized BMD macrophages (Mφs), providing positive control for iNOS (~130 kDa) and arginase-1 (~38 kDa), respectively. After stripping, the upper portion of the membrane was reprobed for ~42-kDa β-actin to confirm equal protein loading.

TIMP-Free ProMMP-9 Produced by B16 TAMs Is Responsible for Enhanced Angiogenesis

To further demonstrate that the proMMP-9 produced by TAMs was responsible in large part for the enhanced angiogenesis-inducing capacity of their secreted products, we employed WT and *Mmp9*-KO C57BL/6 mice implanted with the syngeneic B16-F10 (B16) melanoma cells. Isolation of TAMs from B16 tumors grown in WT and *Mmp9*-KO hosts yielded 3.5 ± 2.0 and 1.9 ± 0.3 × 10^6 TAMs per 1 × 10^8 primary tumor cells, respectively (Table W1). Although lower than the average yields of L929 TAMs, the B16 TAMs from either WT or *Mmp9*-KO mice were of high purity (Table W1) and also exhibited high levels of *Arg1* and *Mrc1* (Figure 5*D*), indicating their M2-skewed phenotype.

Quantification of proMMP-9 production demonstrated that 1 × 10^6 of WT B16 TAMs secreted approximately 3.6 ± 0.9 ng of proMMP-9

Figure 3. Tumor dissemination and development of angiogenic vasculature in human PC-3 prostate cancer xenografts correlates with recruitment of MMP-9–bearing neutrophils. (A) PC-lo/diss (top) and PC-hi/diss (bottom) xenografts were examined for overall histology (left), infiltration by macrophages and neutrophils (middle), and tumor vasculature (right). Some of immunohistochemically-stained (brown) leukocytes and blood vessels are indicated by yellow arrowheads. Bars, 200 μm. (B) Levels of lung metastasis and relative density of TAMs, TANs, and lumen-containing blood vessels in PC-lo/diss *versus* PC-hi/diss tumors. Pooled data (means ± SEM) from two independent experiments, each employing six mice per variant, are presented. *P < .05, **P < .005, ***P < .0001. (C) PC-hi/diss xenografts were double-stained for neutrophil-specific (Ly6G; green) and macrophage-specific (F4/80; red) markers. Bar, 50 μm. Graph: Relative density of TAMs and TANs, quantified in a total of 17 to 30 tumor sections from four tumors harvested in two independent experiments, is presented as fold difference over TAM density (1.0). (D) Left: PC3-hi/diss tumor sections were double-stained for murine MMP-9 (red) and either neutrophil-specific (Ly6G) or macrophage-specific (F4/80) markers (green). Bar, 50 μm. Middle sections depict boxed areas imaged at higher magnification. Bar, 25 μm. Small panels on the right depict examples of double-stained TANs (two top rows) and TAMs (two bottom rows). White arrows point to MMP-9–positive leukocytes with multi-lobed nuclei characteristic of mature neutrophils.

within 48-hour incubation ($n = 3$), while *Mmp9*-KO B16 TAMs did not produce any detectable MMP-9 protein (Figure 5*E*, *top*). However, regardless of their *Mmp9* genetic background, neither WT nor *Mmp9*-KO TAMs secreted detectable amounts of TIMP-1 (Figure 5*E*, *bottom*), thus closely matching the absence of TIMP-1 expression in L929 TAMs (Figure 5*B*, *bottom*).

The production of TIMP-deficient proMMP-9 by WT B16 TAMs correlated with their higher angiogenesis-inducing capacity compared

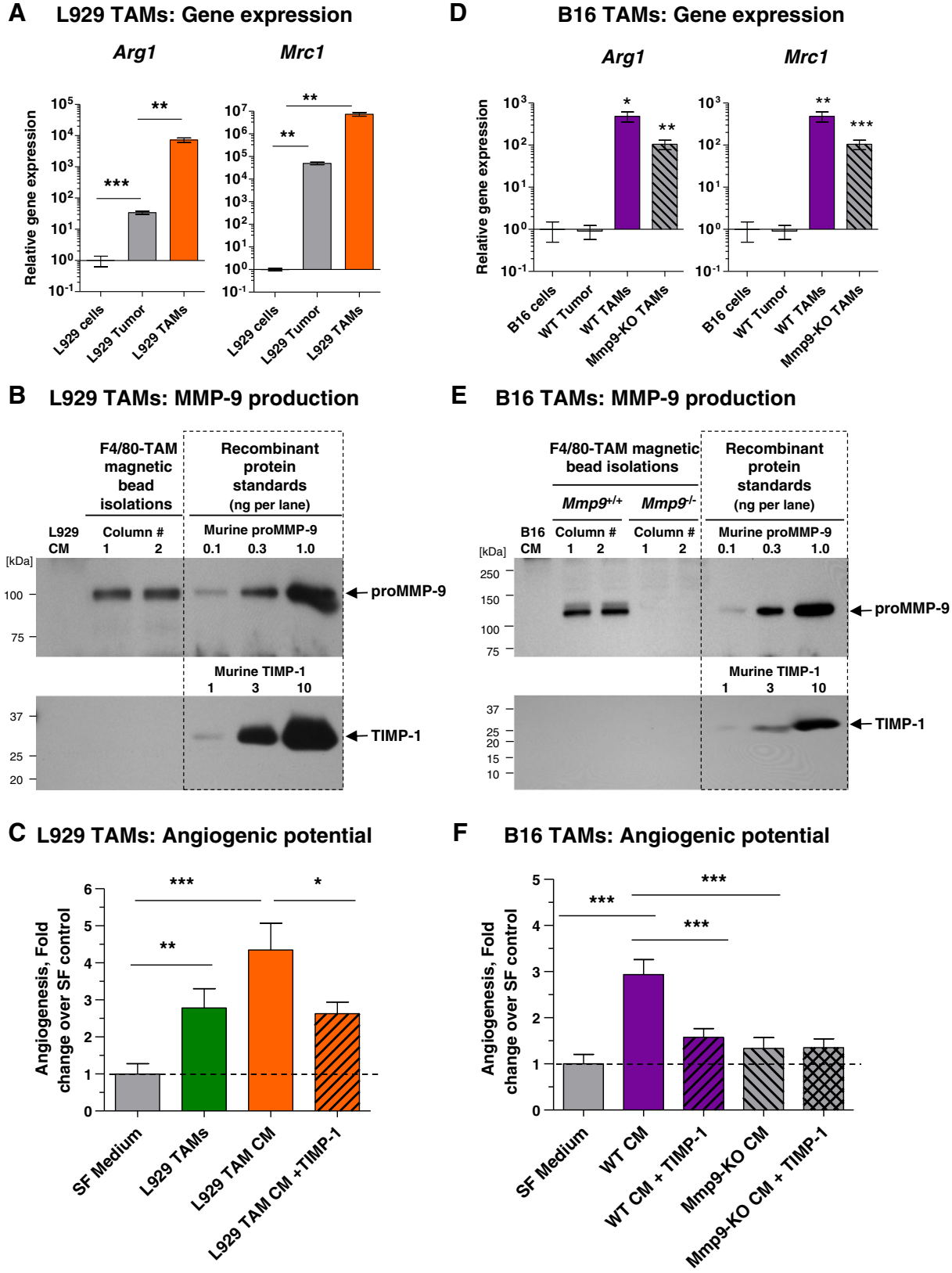

to *Mmp9*-KO B16 TAMs (Figure 5*F*). This enhanced angiogenic potential of CM from WT B16 TAMs was completely abrogated by exogenous TIMP-1, which diminished it to the levels induced by *Mmp9*-KO B16 TAM CM. Importantly, the low levels of angiogenesis induced by *Mmp9*-KO B16 TAMs were not affected by the addition of TIMP-1 (Figure 5*F*), emphasizing the specificity of the TIMP-1 diminishment of angiogenesis induced by WT B16 TAMs.

Angiogenesis-Inducing Capacity of TANs and TAMs in Relation to Their ProMMP-9

To compare angiogenesis-inducing capacities of TAMs and TANs isolated from the same tumor, we turned to the well-established LLC model. LLC tumors were generated in both WT and *Mmp9*-KO C57BL/6 mice. Lineage-specific staining of WT-LLC tumors illuminated both F4/80-positive TAMs and Ly6G-positive TANs, with TAMs distributed more or less evenly throughout the stroma and TANs found more frequently in tighter congregation (Figure 6*A*). However, only WT TANs were simultaneously positive for their Ly6G marker and MMP-9, whereas F4/80-positive TAMs were essentially MMP-9 negative (Figure 6*B*). Highlighting specificity of MMP-9 signal in WT tumors, MMP-9 staining was completely negative in *Mmp9*-KO tumors (Figure 6*C*).

LLC tumor cells induced significant levels of inflammatory cell influx reflected in higher yields of isolated TAMs and TANs compared to B16 tumors, regardless of the *Mmp9* genetic status of hosts (Tables W1 and W3). Isolated LLC TAMs and LLC TANs exhibited their corresponding cell lineage morphology. Thus, HEMA-stained TAMs appeared as relatively large cells (12-20 μm in diameter), with numerous vacuoles within their abundant cytoplasm (Figure 6*D*, *left*). In contrast, much smaller TANs (6-7 μm in diameter) contained multi-lobed nuclei and a small rim of cytoplasm, all characteristic of mature neutrophils (Figure 6*D*, *right*). Both types of isolated tumor-associated leukocytes expressed their respective lineage-specific F4/80 (TAMs) and Ly6G (TANs) markers (Figure 6*E*).

Freshly isolated TAMs and TANs exhibited a dramatic differential in expression of MMP-9, reflected in the bright MMP-9 immunostaining of TANs *versus* barely detectable signal in TAMs (Figure 6*F*). Furthermore, LLC TAMs cultured for 2 days *in vitro* did not induce expression of MMP-9 at levels above background as judged by a double staining for MMP-9 and the general myeloid cell marker CD11b (Figure 6*G*). Western blot analysis of 2-hour LLC TAN releasate *versus* 48-hour LLC TAM CM demonstrated a significant difference in proMMP-9 production (Figure 6*H*), thereby confirming the dramatic differential in cell staining for MMP-9 (Figure 6, *B* and *F*). Quantification of independent TAN preparations ($n = 11$) indicated that 1×10^6 LLC TANs contained on average of 128.0 ± 27.0 ng of proMMP-9 (Figure 6*H*), which is comparable with the amount of proMMP-9 shown for neutrophils isolated from BM (164 ng/10^6 cells; Figure 2*C*). Remarkably, 1×10^6 LLC TAMs produced only 3.4 ± 1.3 ng of proMMP-9 during 48-hour incubation, which was similar to low amounts of proMMP-9 produced by TAMs isolated from both L929 and WT B16 tumors but ~40- to 50-fold lower than amounts of MMP-9 released by LLC TANs. Also consistent with biochemical characteristics of TAMs from the other tumor types, LLC TAMs produced neutrophil-like, TIMP-free proMMP-9 (Figure 6*H*).

Both the intact WT LLC TANs and their releasates were highly angiogenic, yielding angiogenesis at levels exceeding 3.5 ± 0.7 and 3.8 ± 1.0 fold over control levels, respectively ($P < .001$; Figure 6*I*). Importantly, LLC TANs from *Mmp9*-KO mice produced low to non-angiogenic releasates, indicating that the angiogenic potency of WT LLC TANs was almost entirely dependent on their pre-stored proMMP-9. In contrast, intact WT LLC TAMs induced low levels of angiogenesis and only slightly higher levels were induced by their CM (Figure 6*I*).

Within the tumor stroma, MMP-9–positive TANs were almost invariably surrounded by MMP-9–positive fibrillar material (Figure 7*A*), suggesting that TANs deposited their proMMP-9. In contrast, F4/80-positive TAMs were not localized within or near MMP-9–positive stroma unless smaller F4/80-negative cells with neutrophil-like nuclei were in close proximity (Figure 7*B*). These results provided further strong evidence that TANs, not TAMs, are the major source of myeloid cell proMMP-9 in the tumor microenvironment.

Since CM from WT-LLC TAMs appeared to be less angiogenic compared with WT-B16 and L929 TAMs, we thought to determine whether LLC TAMs were particularly sensitive during their *in vitro* incubation to a deficiency in those cytokines that regulate M2-skewed status of macrophages and consequently attenuated their production of proMMP-9. Isolated WT LLC TAMs were incubated with IL-4, a potent inducer of the M2 phenotype. After 48-hour incubation, non-treated and IL-4–treated WT LLC TAMs were analyzed for their angiogenesis-inducing capacity along with freshly isolated cells. Production of

Figure 5. Genetic, biochemical, and functional analyses of TAMs isolated from L929 and B16 tumors. (A) Relative levels of *Arg1* (left) and *Mrc1* (right) expression were determined in isolated L929 TAMs and enzymatically dissociated tumors in comparison with the levels of gene expression in L929 cells in culture (1.0). Pooled data from four independent experiments, each performed in duplicate, are presented. (B) Samples of SF CM from 1×10^5 parental L929 cells (left lane) or L929 TAMs, isolated independently from two tumors on two magnetic bead columns, were analyzed in the same Western blot for MMP-9 and TIMP-1. (C) Isolated L929 TAMs (3×10^4 per onplant) or their SF 48-hour CM was analyzed for angiogenesis-inducing capacity. CM was incorporated alone or with recombinant TIMP-1 (4 ng per onplant). Pooled data from five independent experiments, each employing from four to six embryos grafted with four to six onplants per variant, are presented. Data are means ± SEM. $^*P < .05$, $^{**}P < .001$, $^{***}P < .0001$. (D) Relative levels of *Arg1* (left) and *Mrc1* (right) expression were determined in TAMs isolated from B16 tumors grown in WT or *Mmp9*-KO mice and in enzymatically dissociated WT tumors in comparison with the levels of gene expression in parental B16 cells in culture (1.0). Pooled data from two independent experiments, each performed in duplicate, are presented. (E) CM from 1×10^5 parental B16 cells (left lane) or B16 TAMs isolated from two WT and two *Mmp9*-KO tumors was analyzed by Western blot analysis for MMP-9 and TIMP-1. (F) CM from B16-TAMs isolated from WT or *Mmp9*-KO mice was analyzed for angiogenesis-inducing capacity alone or with TIMP-1. Pooled data from three independent experiments, each employing from four to six embryos grafted with four to six onplants per variant, are presented. Data are means ± SEM. $^{***}P < .0001$.

proMMP-9 was increased by approximately three-fold in IL-4–treated TAMs without any induction of TIMP-1, reaching approximately 10 ng of TIMP-free proMMP-9 per 1 × 10^6 cells (Figure 8*A*). Correspondingly, IL-4– "re-enforced" TAMs exceeded by 3.7 ± 0.7 fold the no-cell control levels during *in vivo* angiogenesis ($P < .001$) and also displayed an enhanced angiogenic potential compared to freshly isolated and non-treated LLC TAMs ($P < .05$ and $P < .005$, respectively; Figure 8*B*).

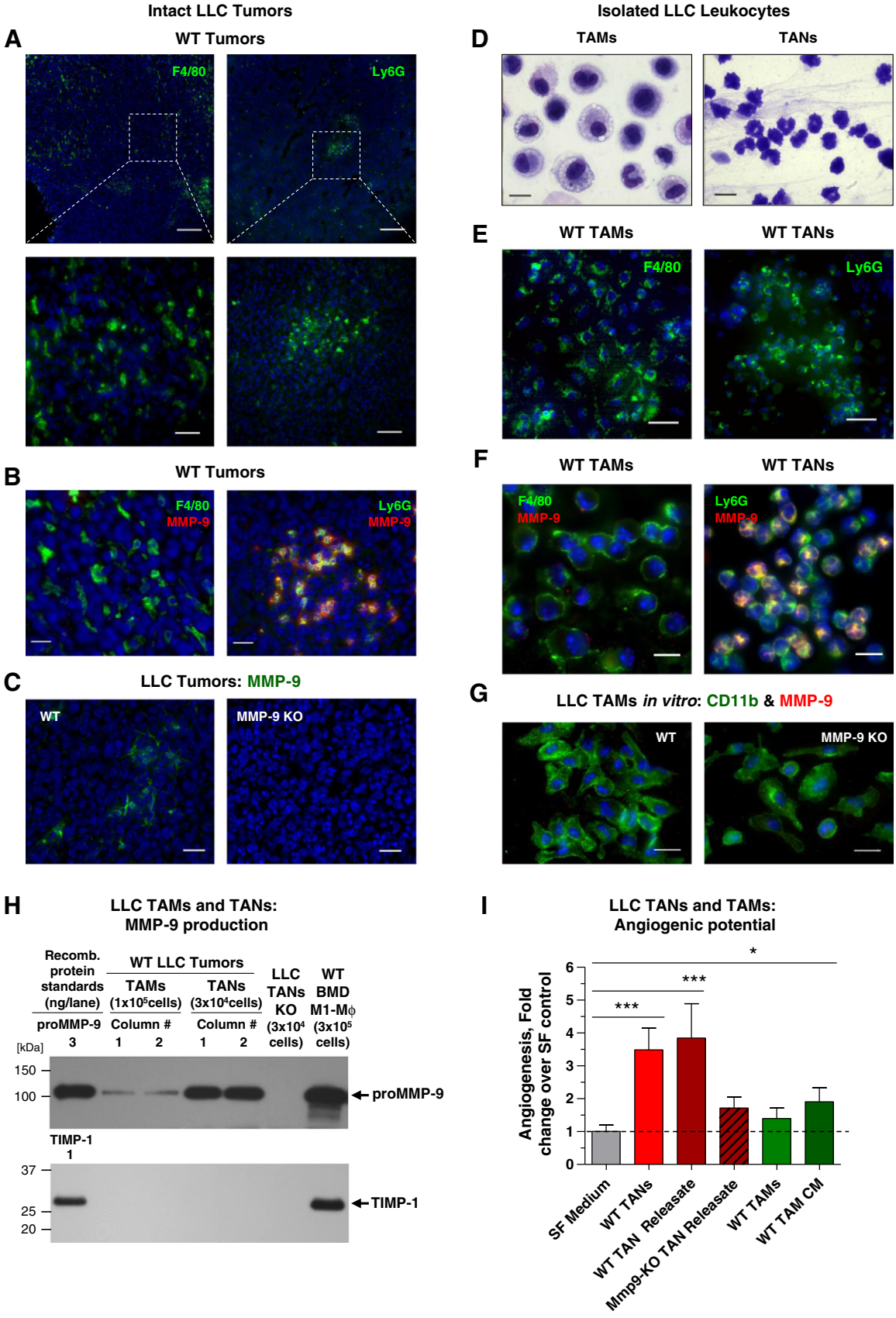

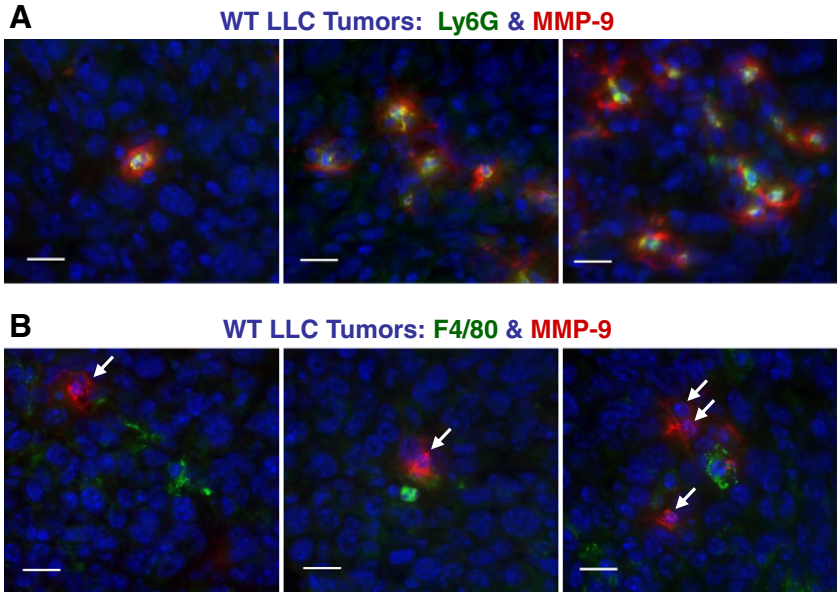

Figure 7. TANs are dominant inflammatory leukocyte type bearing MMP-9. (A and B) Adjacent sections from WT LLC tumors were double-stained for MMP-9 (red) and either Ly6G (green in A) or F4/80 (green in B). Scale bars, 10 μm. Note that the MMP-9 signal in B is associated with cells containing multi-lobed nuclei characteristic of mature neutrophils (white arrows).

These data indicate that regardless of tumor origin (e.g., fibrosarcoma, melanoma, or lung carcinoma), TAMs produce TIMP-deficient proMMP-9 and therefore can induce MMP-9–dependent angiogenesis. However, neither MMP-9 production nor angiogenic potential of TAMs match those of TANs rapidly delivering their abundant pre-stored TIMP-free proMMP-9 at high local concentrations and therefore inducing high levels of tumor angiogenesis.

Microarchitecture of Intratumoral Angiogenic Networks Depends on the Host MMP-9

To relate directly the MMP-9–expressing TANs to a functional angiogenic vasculature, LLC tumors from WT and *Mmp9*-KO mice were analyzed for the presence of mature, lumen-containing blood vessels. Tissue staining for endothelial cells indicated that LLC tumors presented with CD31-positive vascular networks regardless of host *Mmp9* genetic background (Figure 9*A*, *top*). However, analysis at higher magnifications revealed a dramatic underrepresentation of mature, lumen-containing vessels in MMP-9–deficient tumors (Figure 9*A*, *bottom*). Thus, LLC tumors from *Mmp9*-KO mice were infused with small, less than 3 to 5 μm in size, collapsed capillaries without any detectable lumen (Figure 9*A*, *right*), which constituted almost 60% of total CD31-positive structures (Figure 9*B*). In contrast, MMP-9–competent tumors contained four-fold higher fraction of more mature, lumen-containing blood vessels compared to tumors from *Mmp9*-KO mice (Figure 9*B*). Further differential analysis confirmed an underdeveloped organization of angiogenic vessels in the *Mmp9*-KO tumors, which had 85.2 ± 0.1% of vessels with a lumen of less than <10 μm in diameter (Figure 9*C*). In contrast, MMP-9–competent tumors had a significant proportion of angiogenic vessels with lumens of 11 to 20 μm (more than 35%) or >21 μm (more than 15%) in diameter. Quantified against all angiogenic blood vessels, there was a substantial 11.3-fold differential in the density of intratumoral blood vessels containing >11 μm lumen between MMP-9–competent and *Mmp9*-KO tumors (Figure 9*C*).

To investigate whether microarchitecture of angiogenic vessels correlated with the density of pericytes, LLC tumors grown in WT or *Mmp9*-KO mice were double-stained for endothelial (CD31) and pericyte (NG2) markers (Figure 10*A*). Quantification of the ratio of two immunofluorescence signals (NG2:CD31) indicated that the lack of host MMP-9 in LLC tumors correlated with approximately 50% reduction in pericyte density (Figure 10*B*). Furthermore, the lumen-containing vessels were associated with more pericytes in WT

Figure 6. Analysis of TAMs and TANs from LLC tumors grown in WT and Mmp9-KO hosts. (A) LLC tumor from WT mice was immunostained for macrophage F4/80 (left) and neutrophil Ly6G (right) markers (green). Bars, 200 μm (top) and 25 μm (bottom). (B) WT-LLC tumor was double-stained for MMP-9 (red) and either F4/80 (left) or Ly6G (right) markers (green). Bars, 20 μm. (C) Staining of WT and MMP-9 KO LLC tumors for MMP-9 (green). Bars, 25 μm. (D) HEMA staining of TAMs and TANs isolated from WT LLC tumors. Bars, 10 μm. (E) Isolated WT LLC TAMs (left) and TANs (right) stained for macrophage (F4/80) and neutrophil (Ly6G) markers (green). Bars, 25 μm. (F) Isolated WT LLC TAMs (left) and TANs (right) were double-stained for murine MMP-9 (*red*) and either F4/80 (left) or Ly6G (*right*) markers (green), respectively. Bars, 10 μm. (G) LLC TAMs isolated from WT (left) or MMP-9 KO mice (right) were double-stained for myeloid cell marker CD11b (green) and MMP-9 (red). Note the absence of strong MMP-9 signal in TAMs from both tumors. (H) Samples of 48-hour CM from 1×10^5 TAMs or releasates from 3×10^4 TANs isolated from two WT and one *Mmp9*-KO LLC tumor were analyzed by Western blot analysis for MMP-9 and TIMP-1. CM from WT BMD M1 Mφs, producing both proMMP-9 and TIMP-1, provided positive control (right lane). (I) TANs and TAMs were isolated from WT or *Mmp9*-KO LLC tumors and analyzed for their angiogenesis-inducing capacity as intact cells or as TAN releasate and TAM CM. Pooled data from three independent experiments, each employing from four to six embryos grafted with four to six onplants per variant are presented. Data are means ± SEM. *$P < .05$, **$P < .005$, ***$P < .0001$.

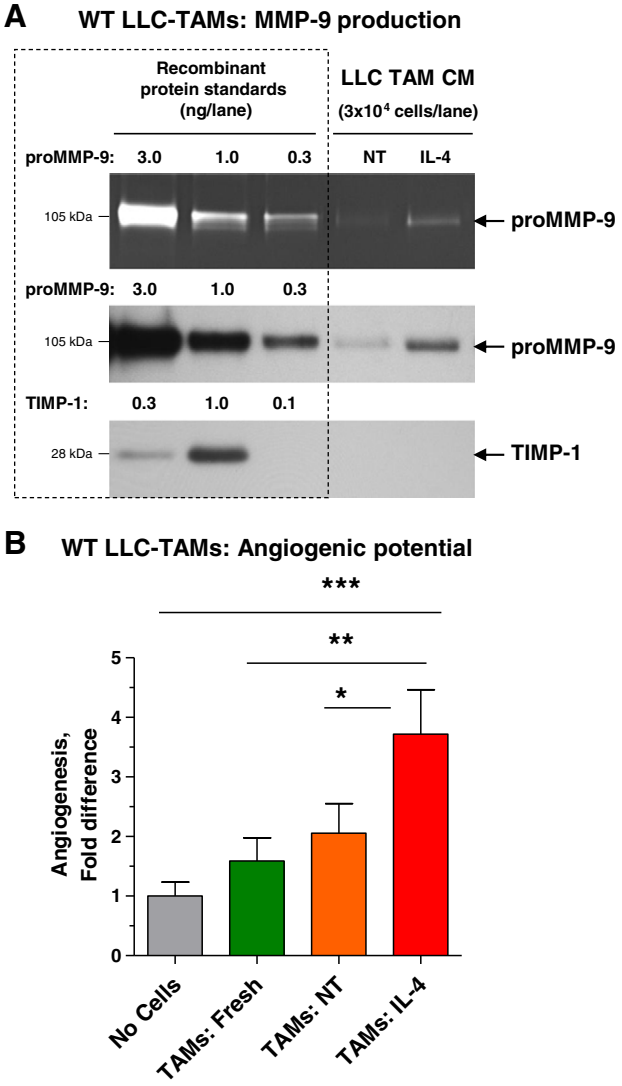

Figure 8. Re-enforced polarization toward M2 phenotype increases proMMP-9 production and angiogenesis-inducing capacity of LLC TAMs. (A) Forty-eight-hour SF CM from WT LLC TAMs, incubated with IL-4 to "re-enforce" the M2 phenotype or left not treated (NT), was analyzed for proMMP-9 and TIMP-1. (B) Freshly isolated TAMs were compared with TAMs treated *in vitro* with IL-4 or left not treated (NT) for angiogenesis-inducing capacity (3×10^4 cells per onplant). Pooled data from two independent experiments, each employing from four to six embryos grafted with four to six onplants per variant, are presented. Data are means ± SEM. $^*P < .05$, $^{**}P < .005$, $^{***}P < .0001$.

tumors than in MMP-9–deficient tumors, where the majority of NG2-positive cells were either scattered within the stroma or located in the vicinity of blood vessels presenting no lumen (Figure 10*C*). Almost identical results were obtained when vascular-associated cells were quantitatively analyzed with another pericyte marker, desmin (Figure 10, *D*–*F*).

It is important to emphasize that the above-described effects of host MMP-9 on tumor angiogenesis and specifically on the microarchitecture of angiogenic vessels and lumen support by pericytes did not depend on the actual presence of TANs (or TAMs) since their yields were comparable between the tumors grown in WT and *Mmp9*-KO mice (Table W3). Taken together, our findings point to TANs as the major contributors of proMMP-9 within the tumor microenvironment, where it induces development of an angiogenic vasculature and sustains its functional microarchitecture.

Discussion

Although high levels of neutrophils and macrophages have been previously associated with tumor angiogenesis and malignant progression in cancer patients [13–15,45–47], xenograft models [10,37,38,48,49], and genetic models of cancer [23,32,33,50], a quantitative investigation of TAM *versus* TAN contribution to the delivery of critical and rate-limiting proangiogenic molecules such as proMMP-9 has not been carried out. Herein, by employing four different primary tumor models, including human prostate cancer xenografts and two syngeneic murine transplant models involving WT and *Mmp9*-KO hosts, we compared functional capacity of TAMs and TANs to produce proMMP-9 and induce MMP-9–mediated angiogenesis. Our results indicate that contrary to conventional notion, it is not TAMs, but TANs that produce abundant TIMP-free proMMP-9, which is readily available for rapid release within the tumor microenvironment and unencumbered activation into a powerful angiogenesis-inducing enzyme.

First, the differentials in levels of tumor angiogenesis and metastasis between high and low disseminating human prostate cancer variants directly correlated with significant difference in the density of TANs, whereas the TAM representation was comparable between the two tumor variants. Furthermore, when the same PC-hi/diss tumors were double-stained for leukocyte lineage-specific markers and MMP-9, a strong signal for MMP-9 was associated only with Ly6G-positive TANs, not F4/80-positive TAMs. Interestingly, in scarce cancer patient–related studies that specifically addressed the MMP-9 localization in the inflammatory leukocytes populating human colon, pancreatic, and hepatocellular carcinomas, most of MMP-9 protein had also been localized to TANs [51–53].

Our previous findings demonstrated the unprecedented ability of PB neutrophils and neutrophil proMMP-9 to induce physiologic angiogenesis [34,36]. Together, these results prompted us herein to quantitatively compare functional capacity of TANs and TAMs to produce proMMP-9 and induce MMP-9–dependent tumor angiogenesis. Paradoxically, TAMs both within tumor tissue and after isolation from either of three histologically different tumor types represented by L929 fibrosarcoma, B16 melanoma, and LLC carcinoma demonstrated near background levels when probed for MMP-9. In contrast, TANs from WT LLC tumors were packed with pre-stored proMMP-9, providing additional evidence for their functional role in the delivery of angiogenic MMP-9 to the site of tumor development. Furthermore, the amount of proMMP-9 produced by isolated TAMs even over extended time periods was 40- to 50-fold lower than that released almost immediately by isolated TANs, a result solidifying the notion that TANs, and not TAMs, are responsible for MMP-9–mediated angiogenesis in the tumor microenvironment, especially at early stages of tumor development.

It appears important to emphasize that although our data identify TANs as a major tumor-associated leukocyte type delivering a specific angiogenesis-inducing molecule, namely TIMP-free MMP-9, into the tumor microenvironment and also corroborate the findings from several neutrophil depletion studies unequivocally demonstrating critical roles of neutrophils in tumor progression [10,33,37,38,54–56], the present study does not dispute the diversified functions of TAMs in tumor growth and angiogenesis, in particular at later stages in cancer progression.

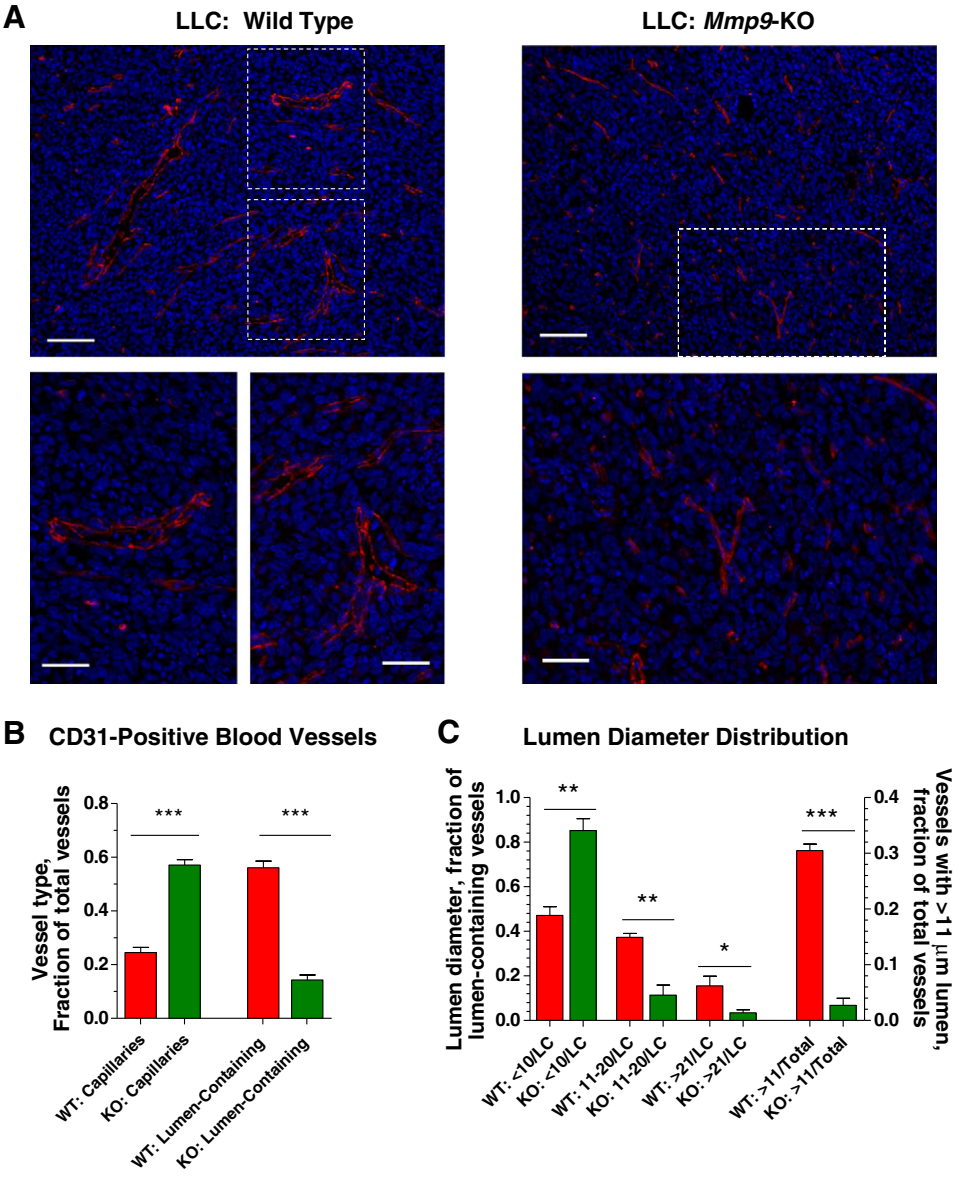

Figure 9. Microarchitecture of intratumoral angiogenic vasculature depends on Mmp9 host genotype. (A) Top: LLC tumors from WT (left) and *Mmp9*-KO (right) mice were stained for CD31 (red). Bars, 100 μm (top) and 50 μm (bottom). (B) Density of CD31-positive lumen-less capillaries and lumen-containing blood vessels was quantified in a total of 45 to 55 tumor images taken from six to eight individual WT and *Mmp9*-KO tumors from three independent experiments. The data are presented as fraction of particular vessel type *versus* total number of vessels. ***P< .001. (C) Distribution of lumen-containing blood vessels according to their lumen diameter. Fractions of intratumoral CD31-positive blood vessels with lumen diameters of <10 μm, 11 to 20 μm, and >21 μm were calculated against total number of lumen-containing vessels (LC). Two bars on the right represent fractions of blood vessels with lumens of >11 μm calculated against total number of intratumoral blood vessels. *P < .05, **P < .005, ***P <.0001.

The present study was also focused on the biology of inflammatory cells producing angiogenic proMMP-9 as well as on the biochemical status of proMMP-9 produced by angiogenesis-inducing leukocytes. Reflecting their full differentiation mode, TANs contained multi-lobed nuclei, a small rim of cytoplasm, and a large MMP-9 cargo, all of which are features of mature neutrophils. Since we showed that BM-isolated neutrophils are also represented mainly by mature MMP-9–loaded granulocytes, it is plausible that the majority of TANs originate from the neutrophils that have egressed from BM to PB and then infiltrated the tumor environment. Cytologic examinations were also consistent with the mature state of TAMs in all four tumor models. Furthermore, positive expression of arginase-1 and macrophage mannose receptor at both gene and protein levels and the lack of iNOS expression allowed us to attribute an M2 phenotype to the isolated TAMs.

According to the data presented herein, the M2-skewed TAMs did not express any detectable TIMP-1 and therefore produced their proMMP-9 as a TIMP-free proenzyme, which is consistent with our previous *in vitro* findings with normal M2-polarized human and murine macrophages [39]. The TIMP-free status of proMMP-9 is an important biochemical characteristic required for unencumbered and rapid activation and high angiogenic capacity of

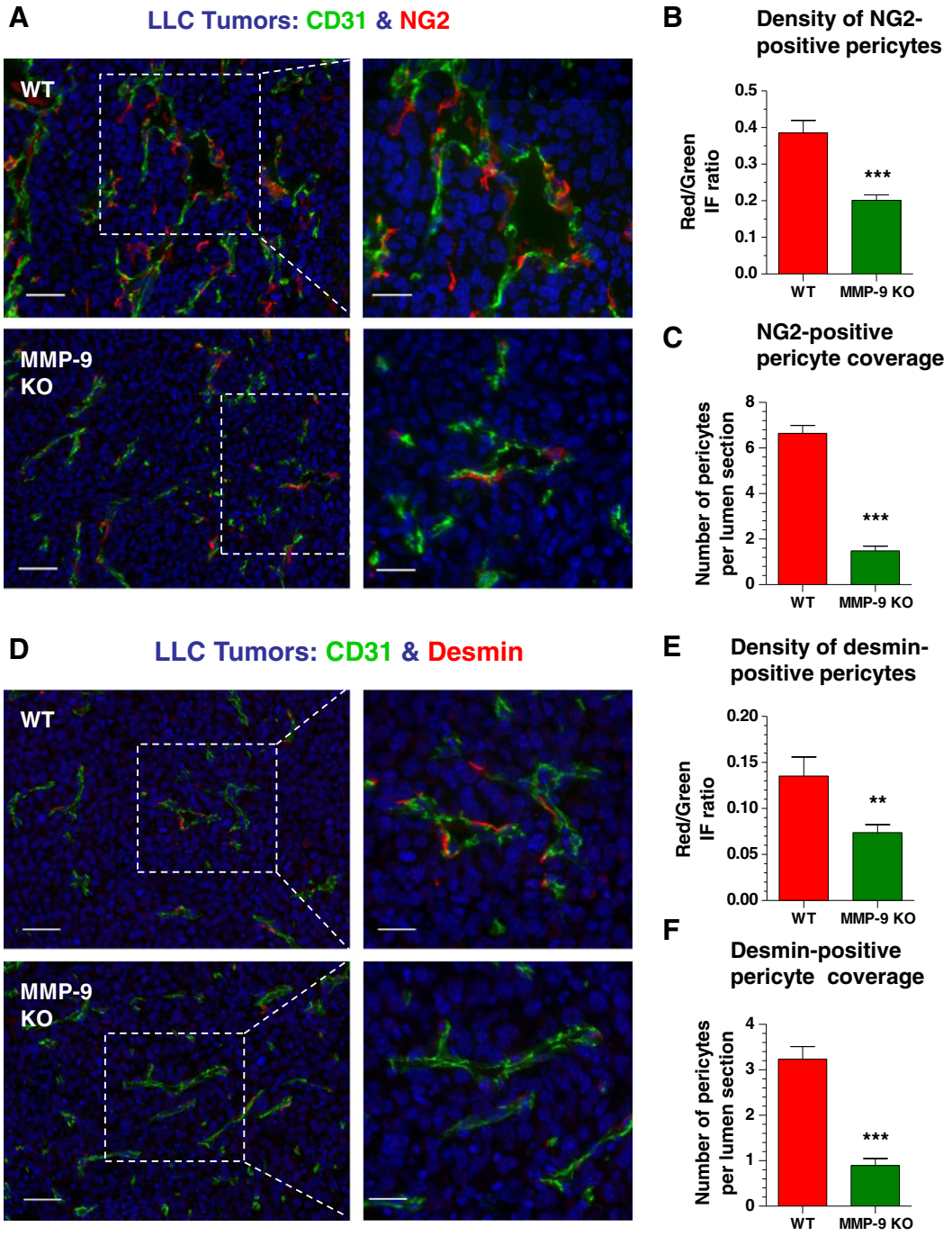

Figure 10. Microarchitecture of angiogenic blood vessels is supported by pericytes in an MMP-9–dependent manner. (A and D) WT and MMP-9 KO LLC tumors were stained for CD31 (green) and either NG2 (A) or desmin (D) pericyte marker (red). Bars, 50 μm (left) and 25 μm (right). (B and E) Pericyte density in LLC tumors grown in WT or *Mmp9*-KO mice was quantified in individual tumor sections as the ratio of IF signal from pericytes (red) *versus* IF signal from CD31-positive vasculature (green). A total of 34 to 38 tumor sections were analyzed in five WT and six *Mmp9*-KO tumors harvested in two independent experiments. ***P< .0001. (C and F) Pericyte coverage was determined as the number of NG2 (C) or desmin (F) positive cells per individual cross-sectioned lumen. A total of 31 and 29 (C) and 56 and 64 (F) vessels were analyzed in WT and *Mmp9*-KO tumors, respectively. ***P < .0001.

naturally produced proMMP-9 [34,36]. In full agreement, TAM proMMP-9 was highly susceptible to inhibition by exogenous TIMP-1, completely losing its relatively low-to-moderate angiogenesis-inducing capacity.

Forced cytokine-induced polarization of human and murine macrophages toward the M2 phenotype *in vitro* is associated with a dramatic down-regulation of TIMP-1 expression after exposure to IL-4, IL-10, or IL-13 [39]. It is likely that, *in vivo*, these cytokines not only negatively control the levels of TIMP-1 production by recruited inflammatory monocytes and mature TAMs but also moderately regulate the levels of MMP-9 secretion. Consistent with this suggestion, IL-4–treated TAMs responded

with increased proMMP-9, but not TIMP-1, production and, correspondingly, with a significantly increased angiogenesis-inducing capacity. These findings strongly suggest that the lack of TIMP-1 production or substantial down-regulation of TIMP-1 gene expression in mature TAMs should constitute a distinguishing feature of M2-skewed macrophages.

Having established that inflammatory TANs were the major source of angiogenic proMMP-9, we further focused our study on the involvement of proMMP-9 in the development and microarchitecture of the induced angiogenic vasculature. Noteworthy, high levels of metastasis in human prostate xenografts coincide with the development of lumen-containing blood vessels and substantial influx of MMP-9–expressing TANs, both in the orthotopic murine model employed herein and also in the chick embryo spontaneous metastasis model [38]. In patients with hepatocellular carcinoma, disease progression directly correlates with tumor infiltration by MMP-9–positive neutrophils and development of sinusoidal vasculature [53]. The notion that MMP-9 competence of inflammatory TANs could determine the lumen-containing status of tumor vasculature was demonstrated in this study by using syngeneic murine tumors developing in MMP-9–deficient hosts. Thus, although the overall levels of tumor angiogenesis were comparable with MMP-9–competent tumors, the tumor vasculature developing in *Mmp9*-KO mice was deficient in lumen-containing vessels and was represented mainly by collapsed capillaries. In contrast, WT tumors, which are infiltrated with MMP-9–delivering TANs, developed blood vessels with lumens of 11 to 20 μm in diameter. Importantly, angiogenic blood vessels with lumens of similar size were also critical for intravasation and dissemination of human epidermoid carcinoma in live animal models [57]. Therefore, it appears that precisely these angiogenic vessel dimensions might be required for accommodating the size and volume of actively intravasating tumor cells.

Our data in the syngeneic LLC tumor model also indicate that MMP-9 competence is required for proper coverage of lumen-containing blood vessels by NG2- and desmin-positive pericytes, which apparently stabilize the vessel wall, thus preventing it from collapsing. This notion is in full agreement with the data showing that inflammatory cell MMP-9 is responsible for pericyte recruitment and support of the angiogenic vessel structure in human neuroblastoma xenografts [25]. However, despite the requirement for vessel wall support, the pericyte coverage of lumen-containing vessels in MMP-9–competent tumors was clearly non-continuous, which could be important for maintaining proper levels of vascular permeability to facilitate intravasation of aggressive tumor cells and their further dissemination. It should be also pointed out that the negative effects of MMP-9 deficiency on tumor angiogenesis in *Mmp9*-KO mice were not attributed to impaired representation of TAMs and TANs in the tumor tissue. Furthermore, these dampening effects were quite pronounced but partial, pointing out that additional and compensatory mechanisms are involved or activated to support tumor growth and metastasis.

In conclusion, our study provides strong evidence that not only is the angiogenesis-inducing proMMP-9 molecule delivered to the tumor microenvironment mainly by TANs and only partially by TAMs but also that a unique TIMP-free proMMP-9 derived from these distinct tumor-associated leukocytes profoundly regulates the microarchitecture of angiogenic blood vessels in a way that facilitates tumor cell dissemination. Our results also suggest that this distinctive form of proMMP-9 could serve as a potential translational target in pathologic conditions associated with acute or chronic tissue inflammation, exemplified herein by neutrophils infiltrating developing tumors and inducing high levels of angiogenesis.

Acknowledgments

The authors are grateful to Chenxing Li for her excellent technical support. The authors thank C. Overall for his generous gift of murine TIMP-1. This is manuscript #21996 from The Scripps Research Institute.

Appendix A. Supplementary data

Supplementary data to this article can be found online at http://dx.doi.org/10.1016/j.neo.2014.08.013.

References

[1] Mocsai A (2013). Diverse novel functions of neutrophils in immunity, inflammation, and beyond. *J Exp Med* **210**, 1283–1299 [PMCID 3698517].
[2] Ginhoux F and Jung S (2014). Monocytes and macrophages: developmental pathways and tissue homeostasis. *Nat Rev Immunol* **14**, 392–404.
[3] Murdoch C, Muthana M, Coffelt SB, and Lewis CE (2008). The role of myeloid cells in the promotion of tumour angiogenesis. *Nat Rev Cancer* **8**, 618–631.
[4] Mantovani A and Sica A (2010). Macrophages, innate immunity and cancer: balance, tolerance, and diversity. *Curr Opin Immunol* **22**, 231–237.
[5] Qian BZ and Pollard JW (2010). Macrophage diversity enhances tumor progression and metastasis. *Cell* **141**, 39–51.
[6] Mantovani A, Sozzani S, Locati M, Allavena P, and Sica A (2002). Macrophage polarization: tumor-associated macrophages as a paradigm for polarized M2 mononuclear phagocytes. *Trends Immunol* **23**, 549–555.
[7] De Palma M and Lewis CE (2013). Macrophage regulation of tumor responses to anticancer therapies. *Cancer Cell* **23**, 277–286.
[8] Condeelis J and Pollard JW (2006). Macrophages: obligate partners for tumor cell migration, invasion, and metastasis. *Cell* **124**, 263–266.
[9] Ruffell B, Affara NI, and Coussens LM (2012). Differential macrophage programming in the tumor microenvironment. *Trends Immunol* **33**, 119–126 [PMCID 3294003].
[10] Fridlender ZG, Sun J, Kim S, Kapoor V, Cheng G, Ling L, Worthen GS, and Albelda SM (2009). Polarization of tumor-associated neutrophil phenotype by TGF-β: "N1" versus "N2" TAN. *Cancer Cell* **16**, 183–194 [MCID 2754404].
[11] Mantovani A (2009). The yin-yang of tumor-associated neutrophils. *Cancer Cell* **16**, 173–174.
[12] Tazzyman S, Lewis CE, and Murdoch C (2009). Neutrophils: key mediators of tumour angiogenesis. *Int J Exp Pathol* **90**, 222–231.
[13] Dumitru CA, Moses K, Trellakis S, Lang S, and Brandau S (2012). Neutrophils and granulocytic myeloid-derived suppressor cells: immunophenotyping, cell biology and clinical relevance in human oncology. *Cancer Immunol Immunother* **61**, 1155–1167.
[14] Galdiero MR, Garlanda C, Jaillon S, Marone G, and Mantovani A (2013). Tumor associated macrophages and neutrophils in tumor progression. *J Cell Physiol* **228**, 1404–1412.
[15] Tazzyman S, Niaz H, and Murdoch C (2013). Neutrophil-mediated tumour angiogenesis: subversion of immune responses to promote tumour growth. *Semin Cancer Biol* **23**, 149–158.
[16] Folkman J, Watson K, Ingber D, and Hanahan D (1989). Induction of angiogenesis during the transition from hyperplasia to neoplasia. *Nature* **339**, 58–61.
[17] Weinberg RA (2008). Mechanisms of malignant progression. *Carcinogenesis* **29**, 1092–1095.
[18] Hanahan D and Weinberg RA (2011). Hallmarks of cancer: the next generation. *Cell* **144**, 646–674.
[19] Bergers G and Benjamin LE (2003). Tumorigenesis and the angiogenic switch. *Nat Rev Cancer* **3**, 401–410.
[20] Deryugina EI and Quigley JP (2010). Pleiotropic roles of matrix metalloproteinases in tumor angiogenesis: contrasting, overlapping and compensatory functions. *Biochim Biophys Acta* **1803**, 103–120 [PMCID 2824055].
[21] Coffelt SB, Lewis CE, Naldini L, Brown JM, Ferrara N, and De Palma M (2010). Elusive identities and overlapping phenotypes of proangiogenic myeloid cells in tumors. *Am J Pathol* **176**, 1564–1576 [PMCID 2843445].

[22] Coussens LM, Raymond WW, Bergers G, Laig-Webster M, Behrendtsen O, Werb Z, Caughey GH, and Hanahan D (1999). Inflammatory mast cells up-regulate angiogenesis during squamous epithelial carcinogenesis. *Genes Dev* **13**, 1382–1397.

[23] Bergers G, Brekken R, McMahon G, Vu TH, Itoh T, Tamaki K, Tanzawa K, Thorpe P, Itohara S, and Werb Z, et al (2000). Matrix metalloproteinase-9 triggers the angiogenic switch during carcinogenesis. *Nat Cell Biol* **2**, 737–744.

[24] Huang S, Van Arsdall M, Tedjarati S, McCarty M, Wu W, Langley R, and Fidler IJ (2002). Contributions of stromal metalloproteinase-9 to angiogenesis and growth of human ovarian carcinoma in mice. *J Natl Cancer Inst* **94**, 1134–1142.

[25] Chantrain CF, Shimada H, Jodele S, Groshen S, Ye W, Shalinsky DR, Werb Z, Coussens LM, and DeClerck YA (2004). Stromal matrix metalloproteinase-9 regulates the vascular architecture in neuroblastoma by promoting pericyte recruitment. *Cancer Res* **64**, 1675–1686.

[26] Jodele S, Chantrain CF, Blavier L, Lutzko C, Crooks GM, Shimada H, Coussens LM, and Declerck YA (2005). The contribution of bone marrow-derived cells to the tumor vasculature in neuroblastoma is matrix metalloproteinase-9 dependent. *Cancer Res* **65**, 3200–3208.

[27] Du R, Lu KV, Petritsch C, Liu P, Ganss R, Passegue E, Song H, Vandenberg S, Johnson RS, and Werb Z, et al (2008). HIF1α induces the recruitment of bone marrow-derived vascular modulatory cells to regulate tumor angiogenesis and invasion. *Cancer Cell* **13**, 206–220.

[28] Zeisberger SM, Odermatt B, Marty C, Zehnder-Fjallman AH, Ballmer-Hofer K, and Schwendener RA (2006). Clodronate-liposome-mediated depletion of tumour-associated macrophages: a new and highly effective antiangiogenic therapy approach. *Br J Cancer* **95**, 272–281 [PMCID 2360657].

[29] Halin S, Rudolfsson SH, Van Rooijen N, and Bergh A (2009). Extratumoral macrophages promote tumor and vascular growth in an orthotopic rat prostate tumor model. *Neoplasia* **11**, 177–186 [PMCID 2631142].

[30] Zhang W, Zhu XD, Sun HC, Xiong YQ, Zhuang PY, Xu HX, Kong LQ, Wang L, Wu WZ, and Tang ZY (2010). Depletion of tumor-associated macrophages enhances the effect of sorafenib in metastatic liver cancer models by antimetastatic and antiangiogenic effects. *Clin Cancer Res* **16**, 3420–3430.

[31] Zaynagetdinov R, Sherrill TP, Polosukhin VV, Han W, Ausborn JA, McLoed AG, McMahon FB, Gleaves LA, Degryse AL, and Stathopoulos GT, et al (2011). A critical role for macrophages in promotion of urethane-induced lung carcinogenesis. *J Immunol* **187**, 5703–5711 [PMCID 3221921].

[32] Giraudo E, Inoue M, and Hanahan D (2004). An amino-bisphosphonate targets MMP-9-expressing macrophages and angiogenesis to impair cervical carcinogenesis. *J Clin Invest* **114**, 623–633.

[33] Nozawa H, Chiu C, and Hanahan D (2006). Infiltrating neutrophils mediate the initial angiogenic switch in a mouse model of multistage carcinogenesis. *Proc Natl Acad Sci U S A* **103**, 12493–12498.

[34] Ardi VC, Kupriyanova TA, Deryugina EI, and Quigley JP (2007). Human neutrophils uniquely release TIMP-free MMP-9 to provide a potent catalytic stimulator of angiogenesis. *Proc Natl Acad Sci U S A* **104**, 20262–20267 [PCMID2154419. PMCID 2154419].

[35] Pahler JC, Tazzyman S, Erez N, Chen YY, Murdoch C, Nozawa H, Lewis CE, and Hanahan D (2008). Plasticity in tumor-promoting inflammation: impairment of macrophage recruitment evokes a compensatory neutrophil response. *Neoplasia* **10**, 329–340 [PMCID 2288539].

[36] Ardi VC, Van den Steen PE, Opdenakker G, Schweighofer B, Deryugina EI, and Quigley JP (2009). Neutrophil MMP-9 proenzyme, unencumbered by TIMP-1, undergoes efficient activation in vivo and catalytically induces angiogenesis via a basic fibroblast growth factor (FGF-2)/FGFR-2 pathway. *J Biol Chem* **284**, 25854–25866 [PCMID2757987. PMCID 2757987].

[37] Bausch D, Pausch T, Krauss T, Hopt UT, Fernandez-del-Castillo C, Warshaw AL, Thayer SP, and Keck T (2011). Neutrophil granulocyte derived MMP-9 is a VEGF independent functional component of the angiogenic switch in pancreatic ductal adenocarcinoma. *Angiogenesis* **14**, 235–243.

[38] Bekes EM, Schweighofer B, Kupriyanova TA, Zajac E, Ardi VC, Quigley JP, and Deryugina EI (2011). Tumor-recruited neutrophils and neutrophil TIMP-free MMP-9 regulate coordinately the levels of tumor angiogenesis and efficiency of malignant cell intravasation. *Am J Pathol* **179**, 1455–1470 [PMCID 3157227].

[39] Zajac E, Schweighofer B, Kupriyanova TA, Juncker-Jensen A, Minder P, Quigley JP, and Deryugina EI (2013). Angiogenic capacity of M1- and M2-polarized macrophages is determined by the levels of TIMP-1 complexed with their secreted proMMP-9. *Blood* **122**, 4054–4067 [PMCID 3862278].

[40] Conn EM, Botkjaer KA, Kupriyanova TA, Andreasen PA, Deryugina EI, and Quigley JP (2009). Comparative analysis of metastasis variants derived from human prostate carcinoma cells: roles in intravasation of VEGF-mediated angiogenesis and uPA-mediated invasion. *Am J Pathol* **175**, 1638–1652 [PMCID 2751560].

[41] Boxio R, Bossenmeyer-Pourié C, Steinckwich N, Dournon C, and Nusse O (2004). Mouse bone marrow contains large numbers of functionally competent neutrophils. *J Leukoc Biol* **75**, 604–611.

[42] Deryugina EI, Ratnikov BI, Bourdon MA, Gilmore GL, Shadduck RK, and Müller-Sieburg CE (1995). Identification of a growth factor for primary murine stroma as macrophage colony-stimulating factor. *Blood* **86**, 2568–2578.

[43] Deryugina EI and Quigley JP (2008). Chapter 2. Chick embryo chorioallantoic membrane models to quantify angiogenesis induced by inflammatory and tumor cells or purified effector molecules. *Methods Enzymol* **444**, 21–41 [PMCID 2699944].

[44] Van den Steen PE, Dubois B, Nelissen I, Rudd PM, Dwek RA, and Opdenakker G (2002). Biochemistry and molecular biology of gelatinase B or matrix metalloproteinase-9 (MMP-9). *Crit Rev Biochem Mol Biol* **37**, 375–536.

[45] Wislez M, Rabbe N, Marchal J, Milleron B, Crestani B, Mayaud C, Antoine M, Soler P, and Cadranel J (2003). Hepatocyte growth factor production by neutrophils infiltrating bronchioloalveolar subtype pulmonary adenocarcinoma: role in tumor progression and death. *Cancer Res* **63**, 1405–1412.

[46] McLean MH, Murray GI, Stewart KN, Norrie G, Mayer C, Hold GL, Thomson J, Fyfe N, Hope M, and Mowat NA, et al (2011). The inflammatory microenvironment in colorectal neoplasia. *PLoS One* **6**, e15366 [PMCID 3017541].

[47] Senovilla L, Vacchelli E, Galon J, Adjemian S, Eggermont A, Fridman WH, Sautes-Fridman C, Ma Y, Tartour E, and Zitvogel L, et al (2012). Trial watch: prognostic and predictive value of the immune infiltrate in cancer. *Oncoimmunology* **1**, 1323–1343 [PMCID 3518505].

[48] Huh SJ, Liang S, Sharma A, Dong C, and Robertson GP (2010). Transiently entrapped circulating tumor cells interact with neutrophils to facilitate lung metastasis development. *Cancer Res* **70**, 6071–6082 [PMCID 2905495].

[49] Strell C, Lang K, Niggemann B, Zaenker KS, and Entschladen F (2010). Neutrophil granulocytes promote the migratory activity of MDA-MB-468 human breast carcinoma cells via ICAM-1. *Exp Cell Res* **316**, 138–148.

[50] Coussens LM, Tinkle CL, Hanahan D, and Werb Z (2000). MMP-9 supplied by bone marrow-derived cells contributes to skin carcinogenesis. *Cell* **103**, 481–490.

[51] Nielsen BS, Timshel S, Kjeldsen L, Sehested M, Pyke C, Borregaard N, and Dano K (1996). 92 kDa type IV collagenase (MMP-9) is expressed in neutrophils and macrophages but not in malignant epithelial cells in human colon cancer. *Int J Cancer* **65**, 57–62.

[52] Gijsbers K, Gouwy M, Struyf S, Wuyts A, Proost P, Opdenakker G, Penninckx F, Ectors N, Geboes K, and Van Damme J (2005). GCP-2/CXCL6 synergizes with other endothelial cell-derived chemokines in neutrophil mobilization and is associated with angiogenesis in gastrointestinal tumors. *Exp Cell Res* **303**, 331–342.

[53] Kuang DM, Zhao Q, Wu Y, Peng C, Wang J, Xu Z, Yin XY, and Zheng L (2011). Peritumoral neutrophils link inflammatory response to disease progression by fostering angiogenesis in hepatocellular carcinoma. *J Hepatol* **54**, 948–955.

[54] Tazawa H, Okada F, Kobayashi T, Tada M, Mori Y, Une Y, Sendo F, Kobayashi M, and Hosokawa M (2003). Infiltration of neutrophils is required for acquisition of metastatic phenotype of benign murine fibrosarcoma cells: implication of inflammation-associated carcinogenesis and tumor progression. *Am J Pathol* **163**, 2221–2232 [PMCID 1892401].

[55] Scapini P, Morini M, Tecchio C, Minghelli S, Di Carlo E, Tanghetti E, Albini A, Lowell C, Berton G, and Noonan DM, et al (2004). CXCL1/macrophage inflammatory protein-2-induced angiogenesis in vivo is mediated by neutrophil-derived vascular endothelial growth factor-A. *J Immunol* **172**, 5034–5040.

[56] McDonald B, Spicer J, Giannais B, Fallavollita L, Brodt P, and Ferri LE (2009). Systemic inflammation increases cancer cell adhesion to hepatic sinusoids by neutrophil mediated mechanisms. *Int J Cancer* **125**, 1298–1305.

[57] Juncker-Jensen A, Deryugina EI, Rimann I, Zajac E, Kupriyanova TA, Engelholm LH, and Quigley JP (2013). Tumor MMP-1 activates endothelial PAR1 to facilitate vascular intravasation and metastatic dissemination. *Cancer Res* **73**, 4196–4211 [PMCID 3754905].